LAPPEENRANTA UNIVERSITY OF TECHNOLOGY
Faculty of Technology
Department of Mechanical Engineering
Laboratory of Steel Structures

Master's thesis

Modeling of residual stresses and distortion due to welding in fillet welds

Supervisors:

Prof.Timo Björk

M.Sc (Tech) Tuomas Skriko

Hassan Muneel Syed

Lappeenranta, 2013

ABSTRACT

Lappeenranta University of Technology

Faculty of Technology

Mechanical engineering

Hassan Syed

Modeling of residual stresses and distortion due to welding in fillet welds

Master's Thesis

2013

44 Pages, 39 figures, 4 tables

Examiners: Professor Timo Björk

Tuomas Skriko M.Sc (Tech)

Keywords: Residual stresses, fillet welds, fatigue life, localized heating, material behavior, weld toe

Welding has a growing role in modern world manufacturing. Welding joints are extensively used from pipes to aerospace industries. Prediction of welding residual stresses and distortions is necessary for accurate evaluation of fillet welds in relation to design and safety conditions. Residual stresses may be beneficial or detrimental, depending whether they are tensile or compressive and the loading. They directly affect the fatigue life of the weld by impacting crack growth rate.

Beside theoretical background of residual stresses this study calculates residual stresses and deformations due to localized heating by welding process and subsequent rapid cooling in fillet welds. Validated methods are required for this purpose due to complexity of process, localized heating, temperature dependence of material properties and heat source. In this research both empirical and simulation methods were used for the analysis of welded joints. Finite element simulation has become a popular tool of prediction of welding residual stresses and distortion. Three different cases with and without preload have been modeled during this

study. Thermal heat load set is used by calculating heat flux from the given heat input energy. First the linear and then nonlinear material behavior model is modeled for calculation of residual stresses. Experimental work is done to calculate the stresses empirically. The results from both the methods are compared to check their reliability.

Residual stresses can have a significant effect on fatigue performance of the welded joints made of high strength steel. Both initial residual stress state and subsequent residual stress relaxation need to be considered for accurate description of fatigue behavior. Tensile residual stresses are detrimental and will reduce the fatigue life and compressive residual stresses will increase it. The residual stresses follow the yield strength of base or filler material and the components made of high strength steel are typically thin, where the role of distortion is emphasizing.

AKNOWLEDGEMENTS

It has been almost six months since I started this master's thesis work and Thanks to God Almighty that I am going to finish it successfully. I came across many challenging tasks during this period and understood the value of a research project. I am very thankful to my supervisor Professor Timo Bjork who gave me this wonderful opportunity to work in steel structures lab so that I can enhance my abilities in strength analysis of structures and get skills for numerical stress analysis on Finite element Packages. Professor Björk deserves great appreciation for his guidance and time even for small matters despite his many other engagements.

A special thanks to Mr. Tuomas Skriko for all his efforts during the experimental part of this study. I also like to express my gratitude to my fellows with whom I shared a great workplace for six months. Mohammad, Tommi, Markus, Toumas, Jukka and Antti you guys really made this journey a pleasant one. I am thankful to all my friends here in Lappeenranta and back home in Pakistan for their moral support which encouraged me and kept me motivated for the task.

In the end I bow to the two pillars of my life, my parents for everything they have done for me from the day one. I can't express it in words what you meant to me

I dedicate this work to the torch bearers of future.

Hassan Syed

Lappeenranta, 28th June 2013

Contents

List of Figures

List of Tables

NOMENCLATURE

Abbreviations

FEM	Finite element method
GMAW	Gas metal arc welding
UHSS	Ultra high strength steel
LEFM	Linear elastic fracture mechanics
HAZ	Heat affected zone

Symbols

σ	Transverse residual stress
Ar	Argon
CO_2	Carbon dioxide
MPa	Megapascal

1 Introduction

Welding in shipbuilding, aerospace industries, pipe and vessel structures has been employed at an increasing rate for its advantages in design flexibility, cost saving and enhanced structural performance. Welding joints are extensively used in all kinds of fabrication industry such as ships, off–shore structures, steel bridges, pressure vessels and in automobile industry. The quality of these welded structures depends upon the joint efficiency, requirements for water resistance, and low fabrication cost. Residual stresses and distortions are unavoidable in welding, and their effects cannot be disregarded. Fillet welds is one of the types of welded joints mostly used in ships, bridge structures, pressure vessels and piping. Residual stresses are occurring due to preventing the free shrinkage of weld and base material around it. Distortion occurs due to shrinkage which can take place partly. Residual stresses and distortions can occur near the T-Joint due to localized welding process and subsequent rapid cooling [1]. They affect the fatigue behavior during external loading significantly.

This effect of residual stresses may be beneficial or detrimental, depending upon the sign, magnitude and their distribution. Generally tensile residual stresses are detrimental and will reduce the fatigue life of the structure as they increase the fatigue crack growth rate and decrease the threshold value of stress intensity factor, while fatigue strength can be increased by compressive residual stresses and they reduce the crack growth rate [2]. High residual stresses near the weld may increase the growth rate of fatigue crack, causing brittle fracture, or stress corrosion cracking. In addition buckling strength of the structural members can be reduced by distortions in the base plate [1].

There is lot of numerical models available describing welding deformations in butt joint in literature, however very little is available predicting deformations in fillet welds. So predicting welding residual stresses and distortions in relation to design and safety consideration is a relevant task for accurate evaluation of T-joint fillet welds.

1.1 Scope and outline of thesis

The scope of this work is to understand the effect of bending and welding process on fatigue strength of the T-joint specimen. The goal is to find out, which kind of residual stresses they

will cause together on the weld toe of the specimen. This research work calculates the residual stresses and deformations due to localized heating by welding process and subsequent rapid cooling in fillet welds. The pretention of the specimen during welding is one important parameter. The effect of residual stresses due to pretension and welding on cyclic stress and on fatigue life of specimen will be studied. Finite element methods have been used to model and analyze the welded joints. The main focus is on T-Joints but X-Joint will also be studied as reference model. The calculated results will be compared with the experimental results to give an idea about the reliability of the simulated results.

The upcoming part of this paper has been divided into different chapters each addressing a specific domain of the work. The next chapter briefly describes the properties of material under study. Chapter 3 gives a theoretical background of the topic and presents an overview of the relevant work done by different group of researchers. Chapter 4 gives the description for experimental work done during this research and presents the experimental results. FE analysis and its results have been documented in Chapter 5. The next part consists of discussion section in which a brief comparison of experimental and simulation results have been presented. The paper is concluded by a conclusion section in the end.

2 Material and Methods

The material under study is UHSS Optim 960QC. This section gives and insight of the material properties used and methods applied during this research.

2.1 Material properties

The material under study is UHSS Optim 960QC. The Optim QC family of ultra-high strength steels offers high strength and good workshop properties. The average hardness of quenched Optim QC steel grades is slightly over 300 HBW which is much higher than the hardness of S355 structural steels. High hardness and tensile strength also indicate good wear resistance. Following table shows the mechanical properties of Optim 960 QC [3].

Table 1. Mechanical Properties of the material.

Steel grade	Yield strength $R_{p0,2}$ MPa Minimum	Tensile strength R_m MPa Minimum	Elongation A_5 % Minimum	Impact strength longitudinally [3] t °C	Charpy V J/cm^2 Minimum
Optim 900 QC [1]	900	950	8 [4]	-40	34
Optim 960 QC [1]	960	1000	7 [4]	-40	34
Optim 1100 QC [2]	1100	1250	6 [5]	-20	34

2.1.1 Thermal properties

Thermal properties for heat transfer analyses are as follow

Expansion coefficient *a*	6.6e -6
Conductivity *k* W/(m.K)	5.55e -4
Specific heat J/g.K	40.53

2.1.2 Chemical composition

Table 2 Chemical properties of the material.

	Maximum content % (cast analysis)					
Steel grade	**C**	**Si**	**Mn**	**P**	**S**	**Ti**
Optim 900 QC	0.10	0.25	1.15	0.020	0.010	0.070
Optim 960 QC	0.11	0.25	1.20	0.020	0.010	0.070
Optim 1100 QC	0.15	0.30	1.25	0.020	0.010	0.070

In addition, aluminium (Al), niobium (Nb), vanadium (V), chromium (Cr), molybdenum (Mo) or boron (B) may be used either singly or in combination.

Ultra high strength steels have a dual-phase microstructure consisting of bainite and martensitic. The average grain size is in the order of 1µm.

2.2 Welding methods

The most commonly used welding method for UHSS is gas shielded arc welding either with solid wire or a fluxed cored electrode. Here in this study GMAW has been used with Bohler Union X96 as filler wire for welding the joints.

2.3 Research Methods

Validated methods for predicting welding stresses and distortion are required because of the complexity of welding process. It includes localized heating, temperature dependence of material properties and heat source. Finite element simulation has become a popular tool of the prediction of welding residual stresses and distortions. Both empirical and simulation methods were used for the analysis of welded joints. The T-joint fillet welds were studied for residual stresses and distortions experimentally and by finite element methods. The calculations were done using FEMAP as software and NX/Nastran as a solver. The calculated values of stresses and deformations by FE analysis were compared with the experimental values.

3 Theoretical investigation

Methods for predicting welding stresses and distortions are required due to the complexities of welding process which includes localized heating, temperature dependence of material properties, and heat source. Several experimental methods including stress-relaxation, X-ray diffraction, and ultrasonic inspection have been used in the past for the prediction of residual stresses and distortions during welding. Strong computational resources in the modern era have made finite element methods more common for analyzing thermo mechanical behavior in welded structures. Finite element simulation has become a popular tool of prediction of welding residual stresses and distortion. Many researchers have predicted the thermal and mechanical responses in weldments both theoretically and experimentally leading ways to eliminate unfavorable deformations. Finite element simulation of the welding process is highly effective in predicting thermo mechanical behavior. Kumose et al. [4] developed an experimental method to measure angular distortions in T-joint fillet welds with different welding parameters. They also introduced the ways to improve angular distortion. A computation model was designed by Michaleris and DeBiccari [5] which estimated buckling and deformation on complex T-joint fillet welds.

Arnold [6] predicted residual stresses in multi pass fillet welds using the FE code PAFEC. Finch and Burdekin [7] discussed the effects of residual stresses on different kinds of T-joint fillet weld defects using FE code ABAQUS.

The investigation made by T.L. Teng et al. performs thermal elasto-plastic analysis using FE technique to analyze thermo mechanical behavior, evaluating the residual stresses and angular distortions of the T-joint in fillet welds [1]. In their study thermal and mechanical models were studies separately. In thermal analysis 160 load steps complete the heating cycle. The modified Newton-Raphson method was used in each time step for heat balance iteration. In mechanical analysis, thermal loading was used as input obtained from temperature history of thermal analysis. The residual stresses from each temperature increment were added to the nodal point location to determine the updated behavior of model before next temperature increment.

Figure 1 shows the two plate fillet weld used in their model by T.L. Teng et al. plate material is SAE 1020 and the mechanical properties are dependent on temperature history. This work

develops two dimensional symmetrical generalized plane strain model to calculate residual stresses of the T-joint fillet welds using FE-method. Thermal stresses are calculated from temperature distribution of thermal model for each weld pass [1].

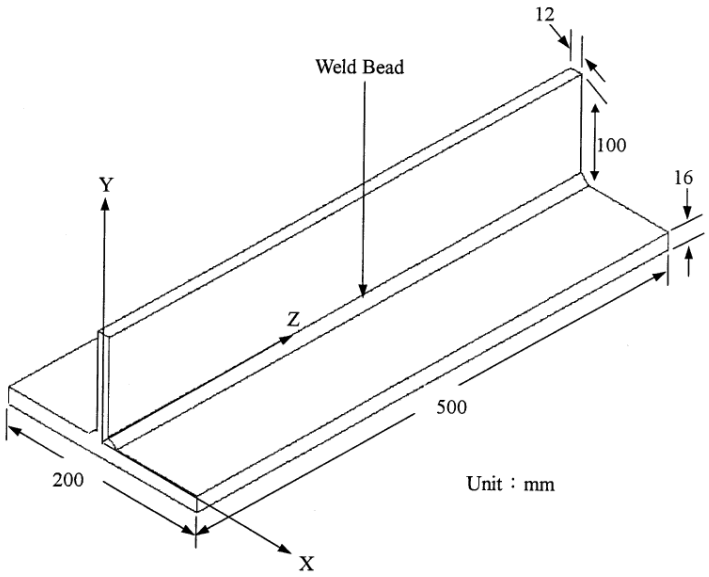

Figure 1. Geometry of T-joint fillet welds

3.1 Transverse residual stresses

A stress acting normal to the direction of the weld bead is known as transverse residual stress, denoted by σ. Large tensile residual stress is produced at the surface of the base plated near the weld toes. The maximum value of residual stress will be σ / yield strength MPa and decreases away from the weld toes. Temperature near the weld bead and heat affected zone changes rapidly with the distance from the heat source. There is a variation in shrinkage through weldment thickness during cooling due to temperature non uniformity so a high tensile residual stress occurs on the surface of the weld toes [1].

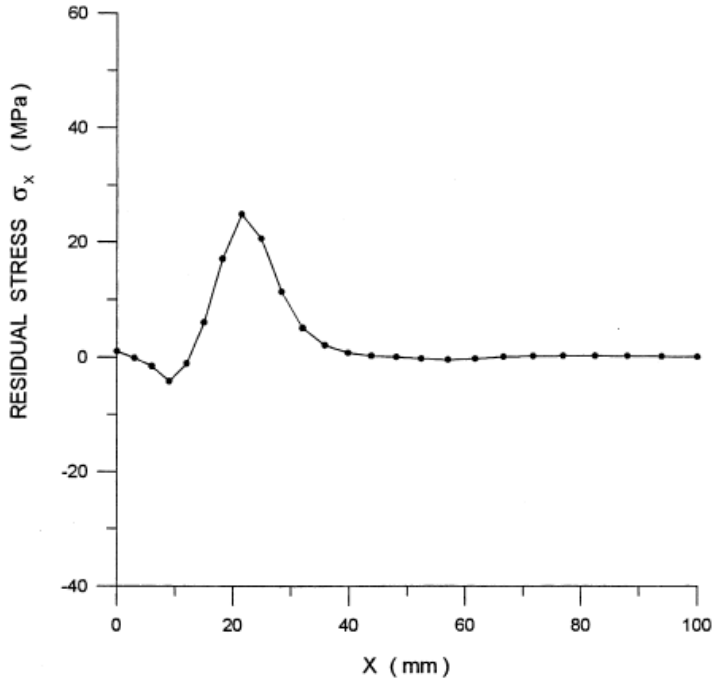

Figure 2. Transverse residual stress distribution along the X direction

3.2 Longitudinal residual stress

Stress acting parallel to the direction of weld bead is known as longitudinal residual stress. It develops from longitudinal expansion and contraction during the welding sequence. A high tensile residual stress appears along the weld line, which become compressive as distance from weld line increases. The residual stress approaches the yield stress of the material which is 110 MPa. In this case the longitudinal stresses are not the focus but the transverse stresses due to shape and loading of the specimen.

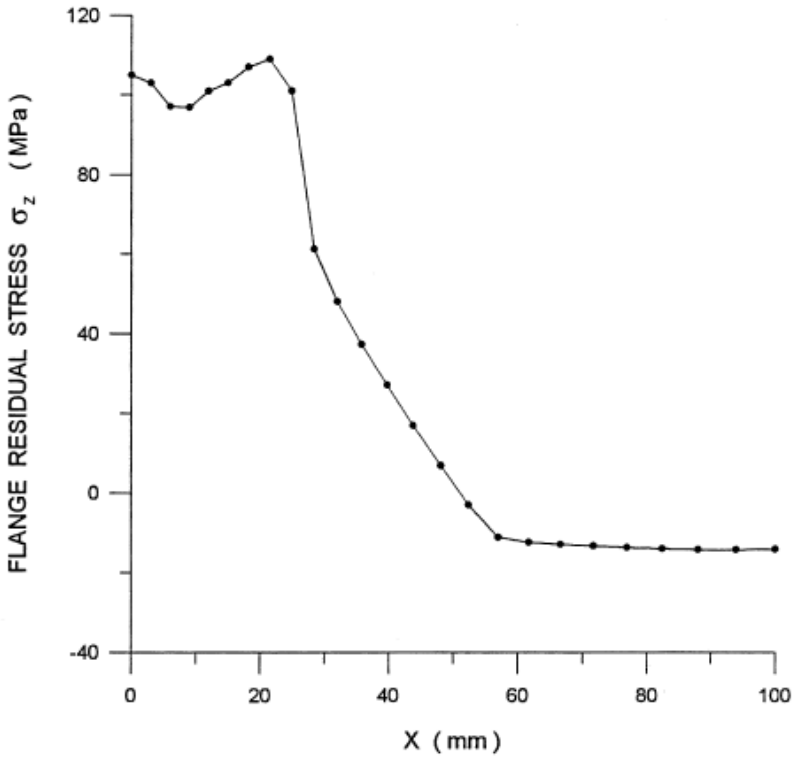

Figure 3 Longitudinal residual stress distribution along the X direction

3.3 Angular distortion

For angular distortion of a T-joint fillet weld the angular change $\Delta\theta$ of the flange for T-type joints is expressed as *a/b*, where *"a"* is the displacement of Y direction and *b* is half of flange length. There are some minor changes in angular distortion with cooling time in T-joint fillet welds which bend the flange up.

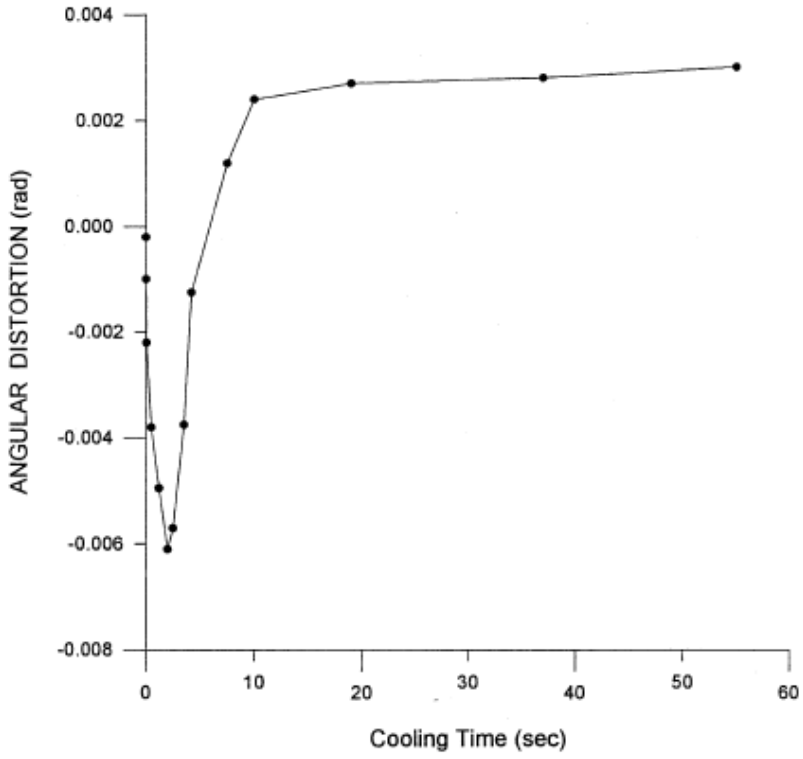

Figure 4. Angular distortion of T-joint fillet welds

This research investigates the effect of restraint conditions and positions on angular distortions and residual stresses. Residual stresses also increases with increasing flange thickness, while they decrease near the fillet weld toe by increasing heat input.

Normally non-linear stress distribution can be separated to stress components.

- σ_m membrane stress
- σ_b bending stress
- σ_{nl} non-linear stress

The membrane stress is equal to the average stress calculated through thickness of the plate. The bending stress is linearly distributed through the thickness of plate. The gradient of bending stress is chosen such that remaining non-linearly distributed component is in equilibrium. The remaining component of stress is non-linear stress peak.

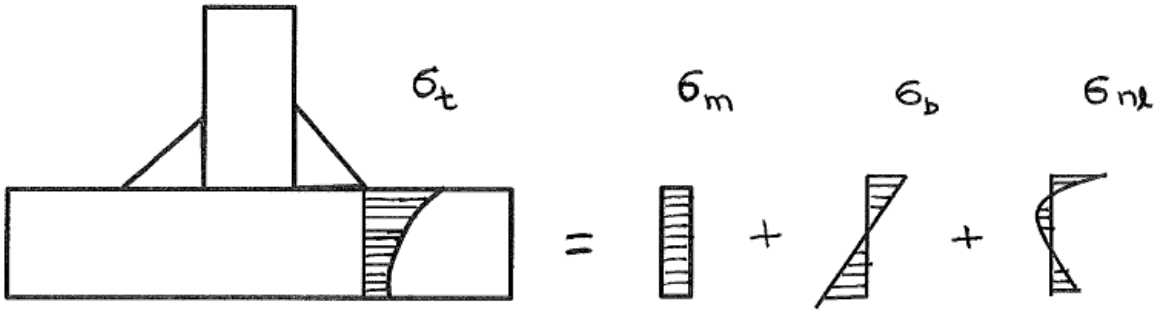

Figure 5. Non-linear stress distribution separated to stress components

A comprehensive FEM analysis of 3D and 2D welding residual stress in T-type fillet welds in high strength steels is done by Ma et al. [8]. The material model assumes temperature dependent of the yield stress, elastic modulus, thermal expansion and Poisson's ratio. Barsoum et al. [9] used the same material model and heat source model and did the transient thermal analysis for the T-fillet weld. Figure 5 shows their analysis where the two welds are simultaneously welded with the same welding conditions

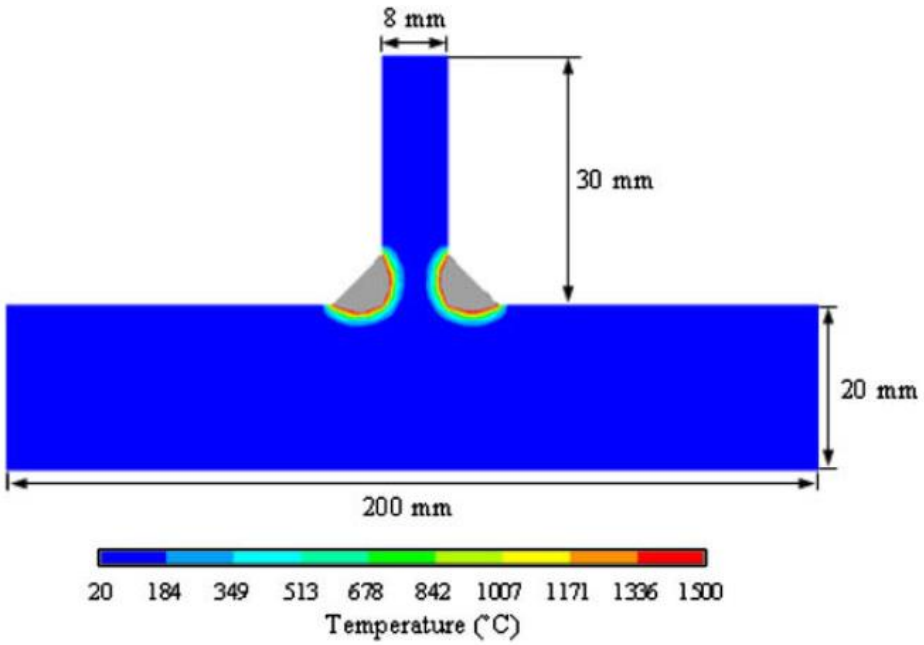

Figure 6 Thermal analysis, fusion zone and isotherms of simultaneous welding of T-fillet weld **[9]**

Barsoum et al. compared their longitudinal and traverse residual stresses with the 2D and 3D predictions made by Ma et al. The predicted residual stresses show good agreement.

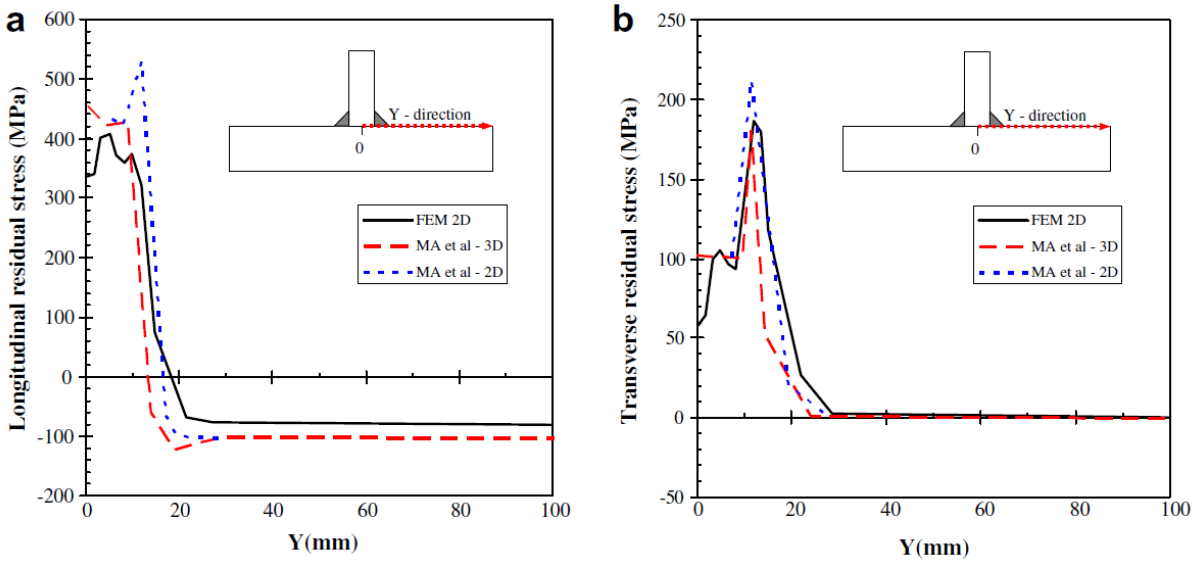

Figure 7. Residual stress prediction and comparison with Ma et al. for fillet weld **[9]**

3.4 Determination of welding residual stresses

The development of residual stresses in steels with phase transformation could be explain by the models of Wohlfahrt and Nitschke-Pagel [10]. In Figure 7-left, thermal contraction and hindrance of shrinkage cause tensile stresses in austenite. These stresses can be as high as the yield strength of austenite and respective temperatures. By decreasing the temperature and beginning of phase transformation for respective steels, the tensile stress relaxes and approaches to zero and becomes compressive. Depending upon the transformation temperature, tensile (curve 1), zero (curve 2) and compressive (curve 3) residual stresses could be developed during cooling

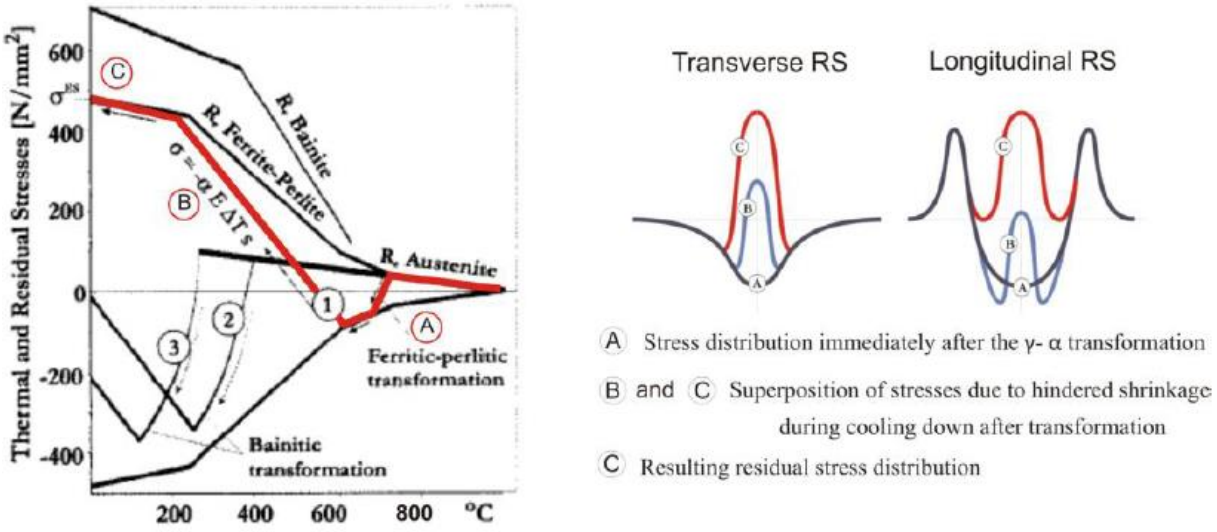

Figure 8. Residual stress development due to phase transformation and shrinkage **[10]**

Experiments were carried out by Farajian [11] on different types of steel with yield strength between 300 and 1200 MPa. Steel plates of S235JRG2, S355J2G3, P460NL, S690QL and S960QL were prepared and then were welded together. The surface residual stresses were measured by x-ray diffraction techniques.

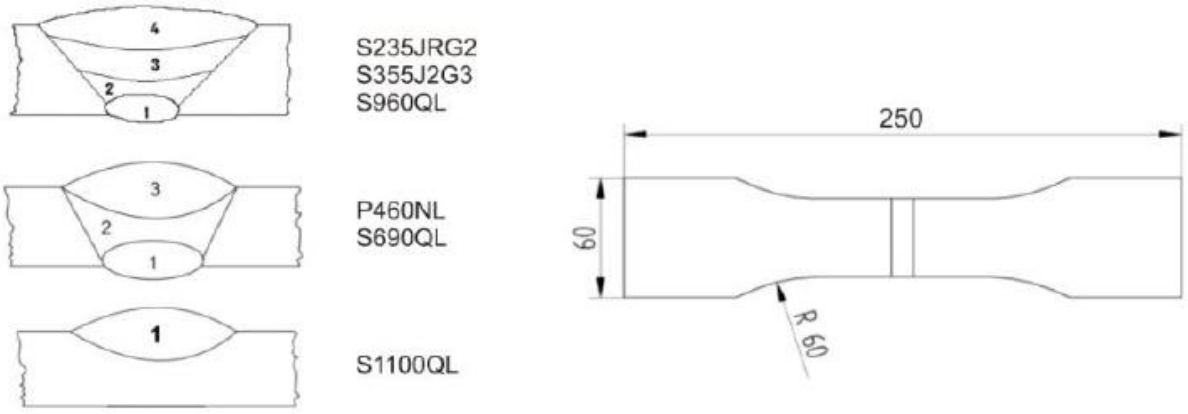

Figure 9. Cross section of welds and size of the small specimen

The surface residual stresses for all welded specimens with different base material in transverse and longitudinal directions are presented in Figure 9. The distribution profiles are mean values of the measurements on 15 specimens for each base material. The shape and characteristic features of measured residual stress profiles in figure 9 are in good agreement with the schematic model in Figure 7. The maximum residual stresses in the welds are not as high as yield strength in the model because temperature at which phase transformation begins the shrinkage process could be disturbed and different residual stresses could be developed [11].

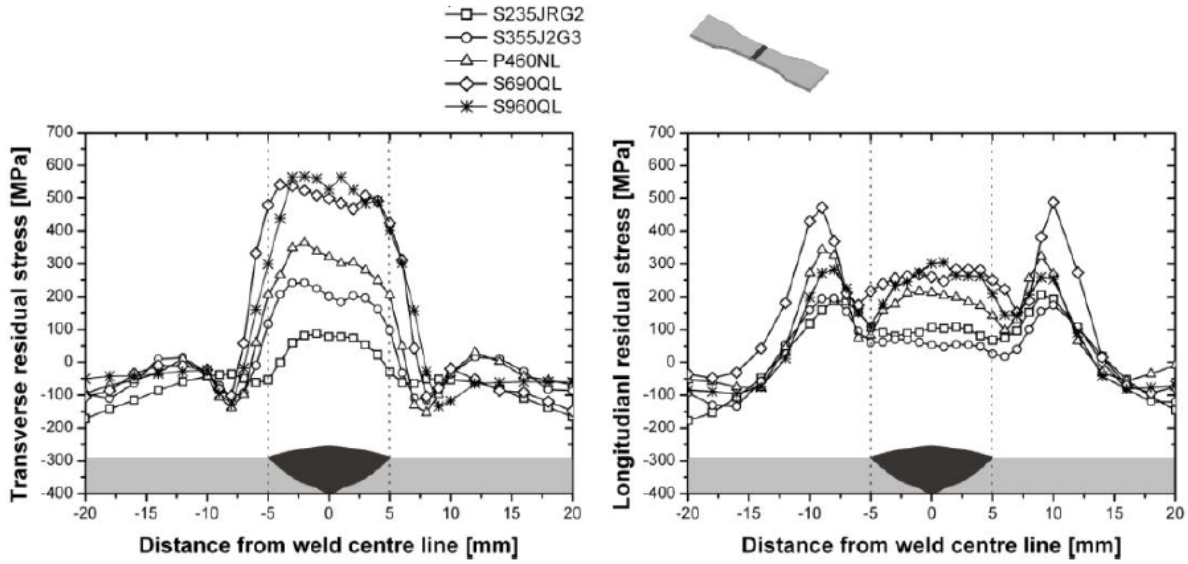

Figure 10. Residual stress distribution in welded specimens in transverse and longitudinal directions

3.5 Residual stress impact on fatigue life of welded joint

Residual stresses can have a significant effect on fatigue performance of the welded joints. A fatigue crack has poor growth under a predominantly residual stress field. Fatigue cracks growing through weld residual stress field have got significant attention of the researchers since long. Glinka presented an analytical approach for fatigue crack growth prediction while studying the effect of residual stresses on low alloy steel welds [12]. Forman-Wheeler model crack retardation effect under variable amplitude loading. Theoretical results seem more realistic when stress ratios and stress intensity ranges were considered depicting residual stress effect [13]. Recent Publications made in IIW have discovered both beneficial and detrimental effects of weld residual stresses on fatigue life. Barsoum [14] has developed welding simulation procedures, crack growth and residual stress mapping routines for weld analysis.

A quantitative assessment of influence of residual stresses on fatigue life can be made by mean stress approach which is based on the linear elastic fracture mechanism using NASGRO equation which shows the residual stresses by calculating additive residual stress approach in which the superposition principle [15]. In this method range of effective stress intensity factor does not change, but the local stress ratio changes which ultimately change the crack growth rate.

Both initial residual stress state and subsequent residual stress relaxation need to be considered for accurate description of fatigue behavior. When initial residual stress and applied stress exceeds the material yield strength, the effective residual stress starts to reduce with complete stress relaxation occurring when the combined stress reaches 1.9 times the material yield strength [15].

There are several methods available to measure stress intensity factor for a given crack like closed form solutions for simple geometries, weight function solution, finite element approach for complex geometries and some hybrid methods. Finite element methods are used to obtain stress intensity factor for crack geometries for which manual solution is not possible. Some FEA software like ABAQUS provides finite element techniques that do not require crack models. There might be a change in stress intensity factors due to residual stresses. Dong and Hong [16] proposed displacement controlled K solution for considering welding residual

stresses. There is a significant difference in K behavior between load controlled and displacement controlled conditions in a pure bending state.

The nominal stress approach is the most common analysis approach for welded structures. Nominal stress and weld classification is sometimes difficult to apply on complex geometries under complex loading. It is important to include residual stresses in the assessment of fatigue life of a welded joint especially when they are compressive. Linear elastic fracture mechanics (LEFM) can provide better accuracy than the nominal stress approach in fatigue prediction. But computational effort and input parameters in LEFM are challenges in this regard.

4 Experimental Test

Experimental part of this research work is performed in Laboratory of Steel Structures, Lappeenranta University of Technology. The basic idea was to measure and calculate stresses during welding with empirical methods and then compare them with the simulated FEA analysis. The main specimen is prepared by putting measuring devices and welded with welding robot. This section illustrates the experimental setup and results taken from it.

4.1 Setup

The apparatus used for this experimental setup includes a base material which is the specimen, two fillet welds which are to be welded on the base plate, two strain gauges, four thermocouples, loads for preloading, and the welding robot. Gas metal arc welding is used to weld the specimen. The shielding gas is Ar + 18 % CO_2 and Böhler Union X96 is used as filler wire. The welding parameters used for both welds are as follow

	Voltage U (volts)	**Current I (A)**	**welding speed v (mm/s)**
Weld 1	31.5	277	6.2
Weld 2	31.5	281	6.2

The Heat input used is 1KJ/mm and established throat thickness was 5mm.

Strain gauges are mounted 50 mm away from the weld toe on both sides of the weld because they can melt during welding if we place them on the weld toe. Four thermocouples are placed on the weld toe to read the temperature, two on each side of weld as shown in the schematic of experimental setup in Figure 7.

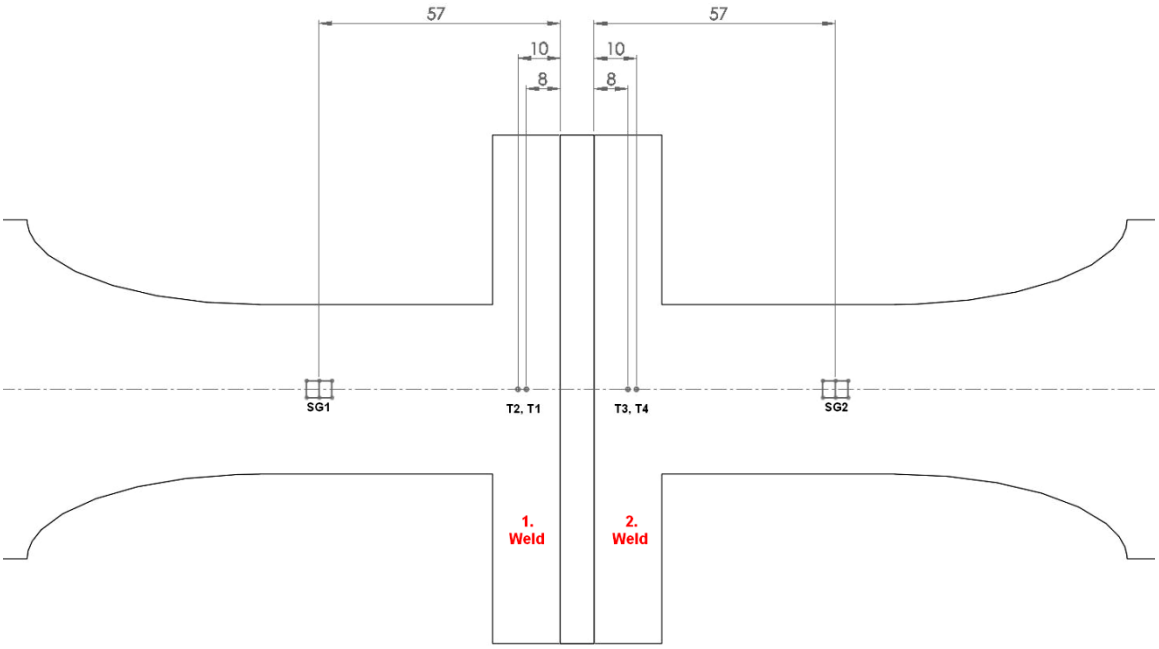

Figure 11. Schematic of experimental setup for measuring the residual stresses during welding

Following Figure 8 shows the experimental setup and working in the laboratory during the experiment. As it can be seen the specimen is clamped on the welding bed. Strain gauges and thermocouples are mounted as shown in the above schematic diagram. The wires are fed to the measuring device which measures the data and send it to the computer for storage and further processing. Welding robot is used during this experiment. It is necessary to mention here the welding was done one by one for both of the welds on both sides of specimen in contrast to the finite element model where the thermal load is applied simultaneously on the both sides of the weld.

Figure 9 shows both the complete welds left for cooling them and reading the residual stresses produced during cooling down of the specimen. Welding is done one by one on both sides of the weld specimen that means one weld was given time to cool down before next weld.

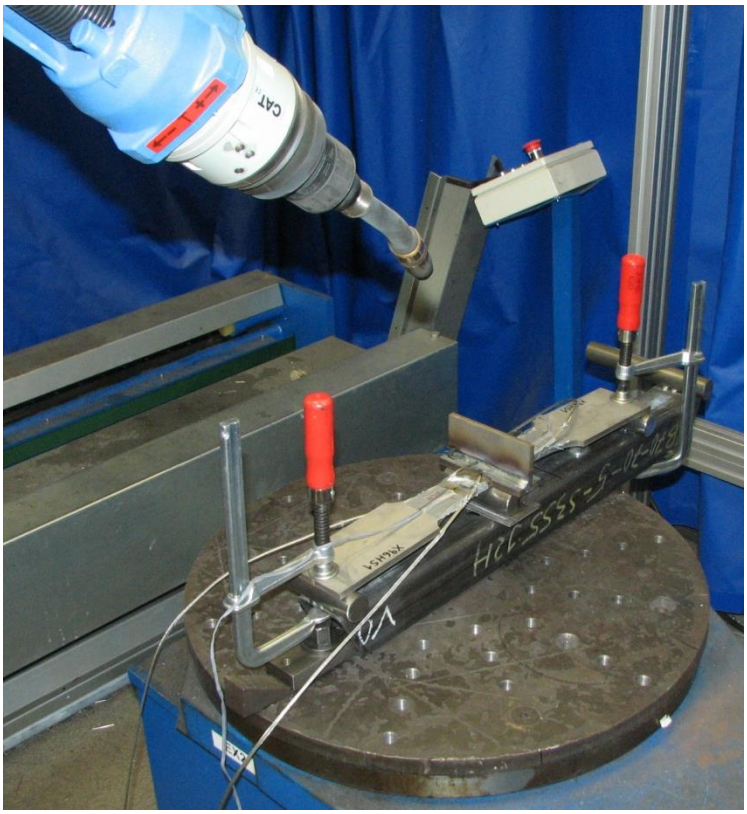

Figure 12 Experimental setup for welding the specimen mounted with gauges and thermocouples

Factor by which elasticity modulus (left) and yield strength (right) changing with temperature

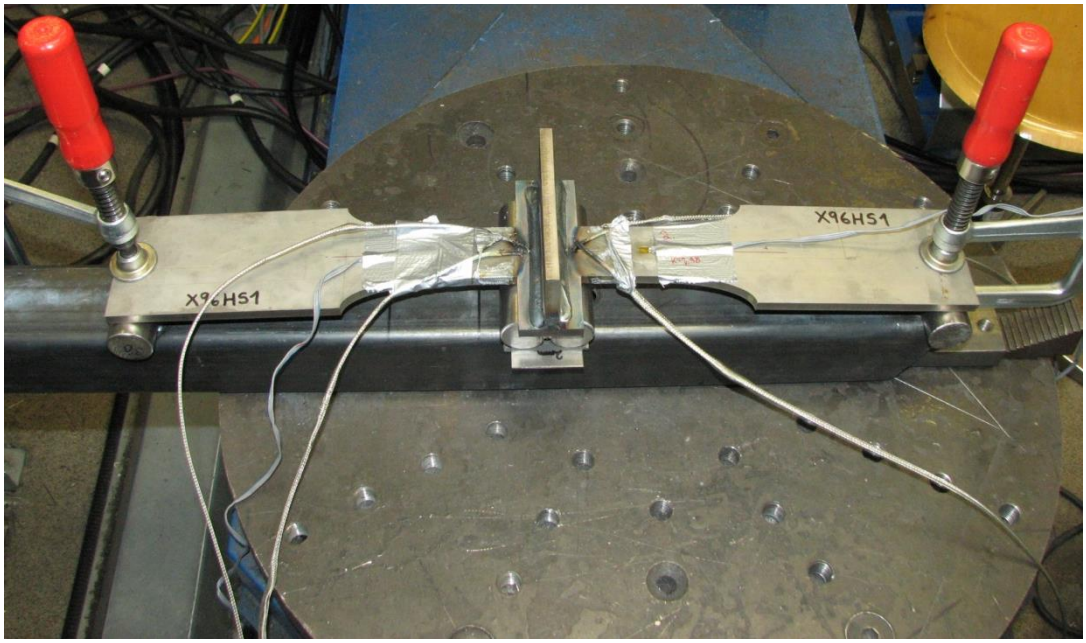

Figure 13 Specimen after welding during cooling time

4.2 Experimental Results

The test data from strain gauges and thermocouples are taken in the form of volts from the reading device and then they are converted into respected stress and temperature values using Hook's law. Stresses from gauges are normal stresses in x-direction. Here the plots of x-direction stresses and temperature have been presented.

Figure 10 shows the plot of x-direction stress distribution 50 mm away from the weld toe. The maximum stress value read by gauge 1 is around 360 MPa. At the beginning this 350 MPa came from the preload. Then there was the first welding part (approx. time step 300) and after first welding the stress value decreased to 270 MPa. The second welding was done at time step 2400 (see the peak value) and after that stress values returned back to 270 MPa. At the end preload was released and stress value dropped to near zero.

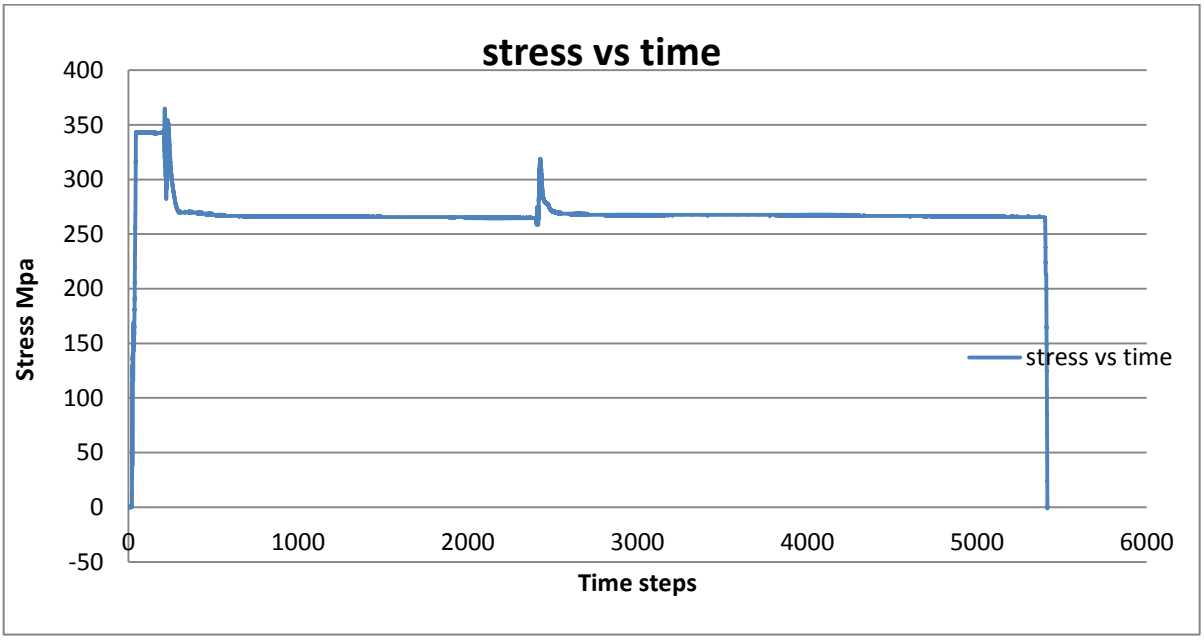

Figure 14 X-direction stresses from gauge 1

Figure 11 shows the plot for x-direction stress distribution on the other side of the weld toe. Here the maximum stress value is 375 MPa. The stress distribution pattern is almost same in Figure 10 and Figure 11. Initial stress values are with the pre load without welding. Then the

stress reaches to maximum value during welding and it remains constant after welding and finally drops down to zero after removing the preload.

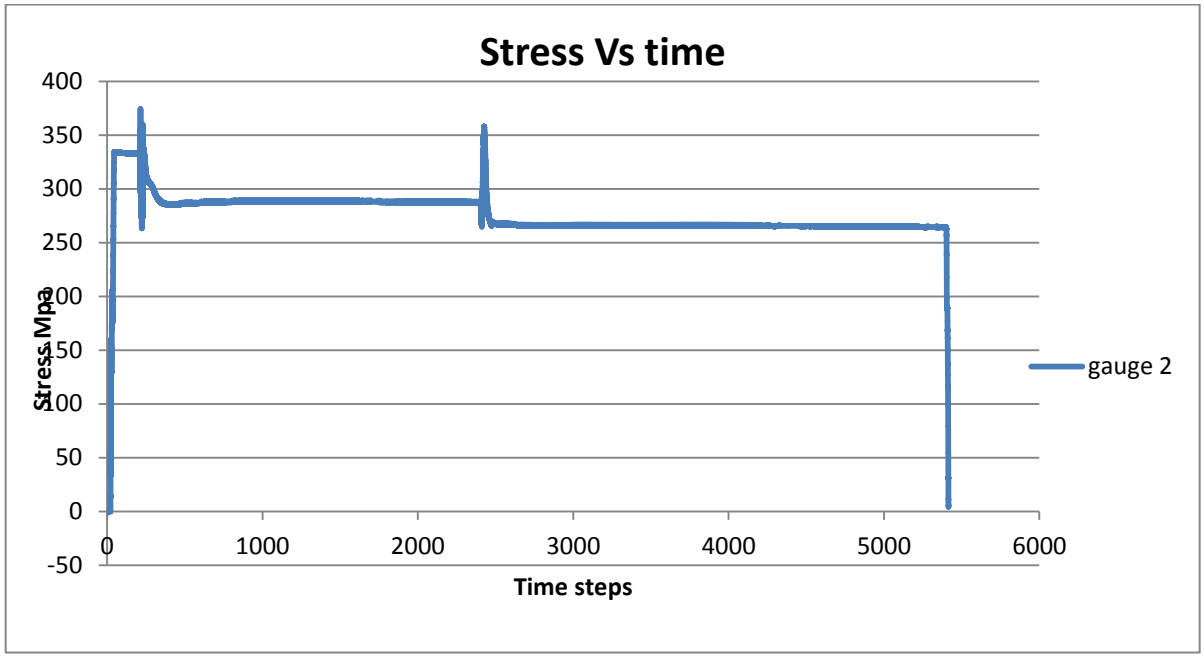

Figure 15 X-direction stresses from gauge 2

Figure 12 shows the temperature variations T1 from thermocouple 1 at the weld toe. The maximum value for temperature is almost same near weld toe as found in the FE model.

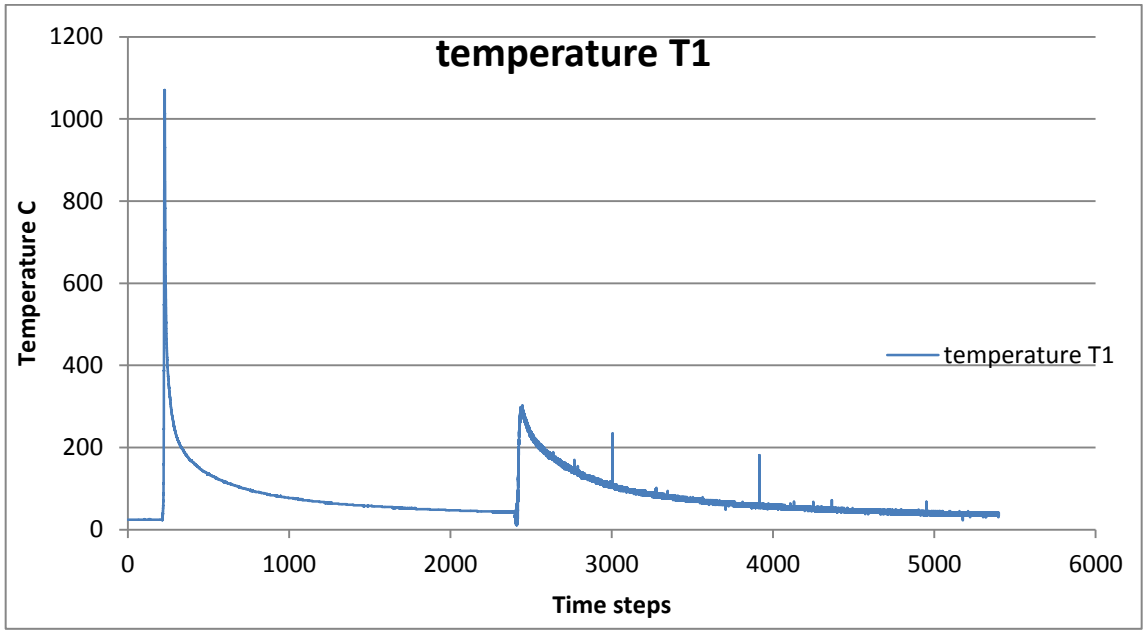

Figure 16 temperature T1 at the weld toe

Figure 13 shows the temperature T4 near the weld toe. The temperature variation is low in the beginning and its start rising during the weld and reaches to its maximum position at the weld toe. The temperature drops again to minimum values while cooling down the weld.

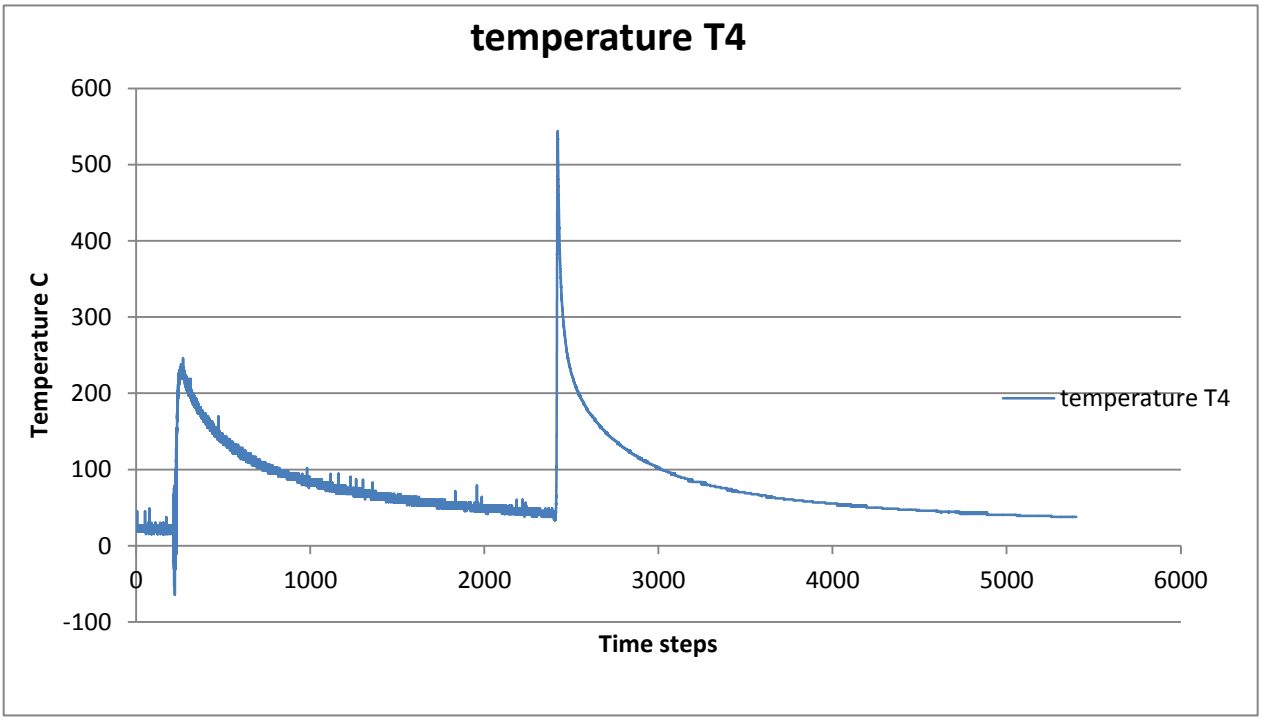

Figure 17. Temperature T4 near the weld toe

5 FEA Analyses

Finite element analysis is done using the software FEMAP and NASTRAN as solver. The software has a friendly user interface and accurate for simple and complex calculations. Specimen model is built in FEMAP and stress contours and plots were taken after simulation.

5.1 Geometry

The geometry was built in Solid Works and imported into FEMAP for analyses.

The following is the isotropic view of the T-joint fillet weld shown in Figure 14.

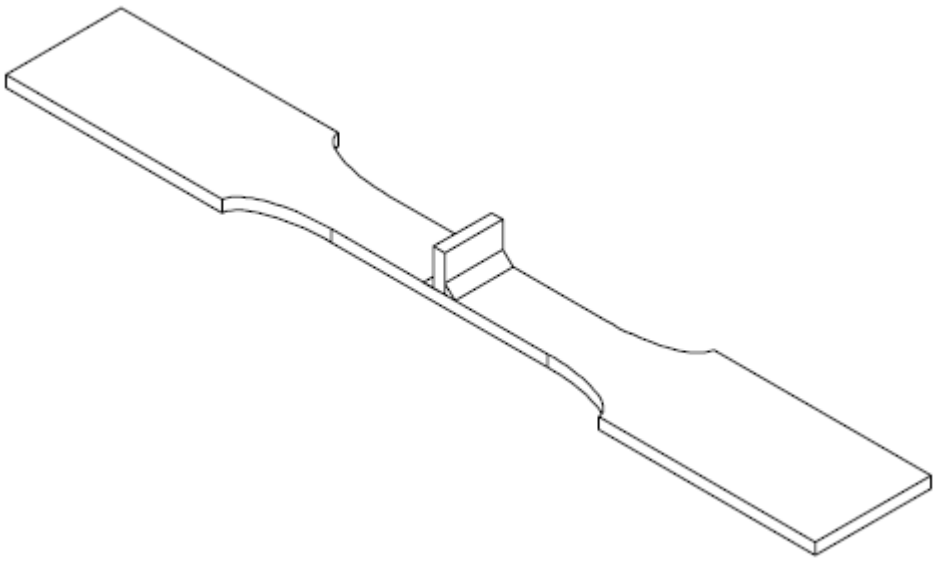

Figure 18. Isotropic view of the T-joint fillet weld

The length of the weld is 40 mm and the width of the weld toe is 11.2 mm

The dimensions for this fillet weld joint are shown in the following figure more precisely.

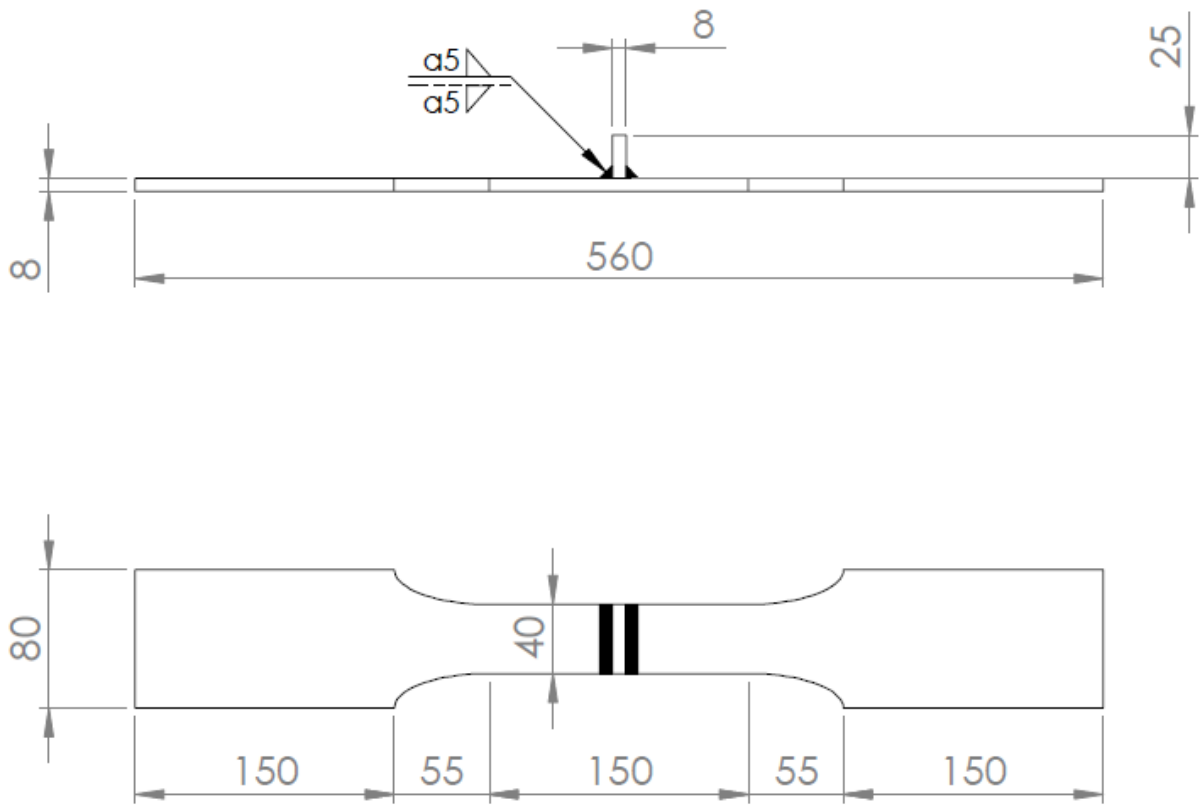

Figure 19. Dimensions for the T-joint fillet weld

5.2 Material properties

The material used in the modeling of these welding joints is UHSS Optim 960QC.

Other welding parameters are:

- Base material: Ruukki Optim 960QC
- Filler metal: Böhler Union X96
- Shielding gas: Ar + 18 % CO_2
- Heat input: 0.8 kJ/mm

5.3 Modeling cases

In this study following modeling cases will be modeled and studied for residual stresses and distortions. The main focus is on T-joint fillet welds but x-joint will also be modeled for reference.

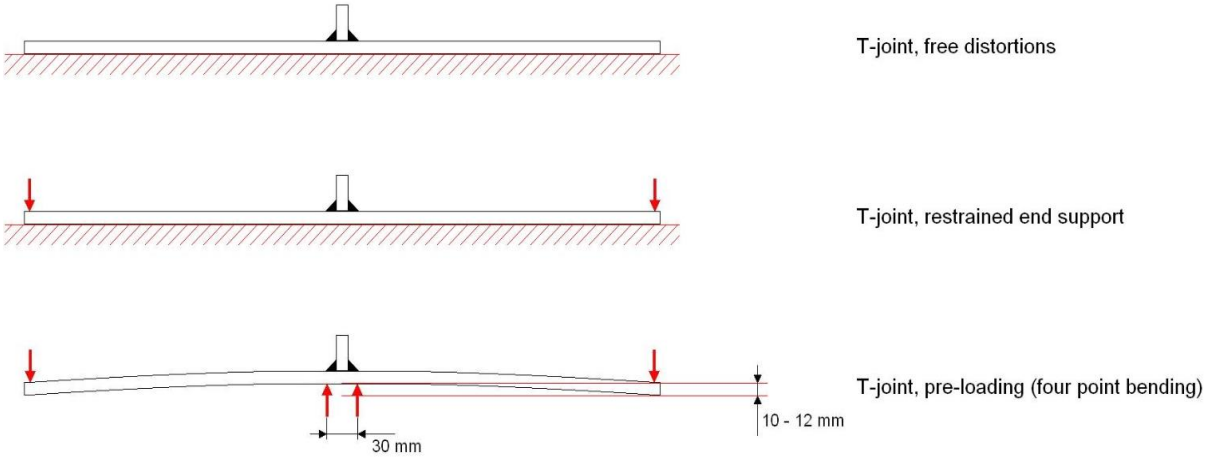

Figure 20 modeling cases

The first case is without any constraint. It shows the free T-joint without any forced displacements. The second case is with constraints at the both ends. The third case shows the forced displacements in the joint with transverse loads on it.

5.4 Meshing and mesh size

After setting material properties mesh was applied on the geometry. The element type used in this case is trigonal and 3D solid element property type is chosen for analyses. Mesh size along curve was used to specify the element size and the spacing between them along the curve. In the first case number of elements are 7505.

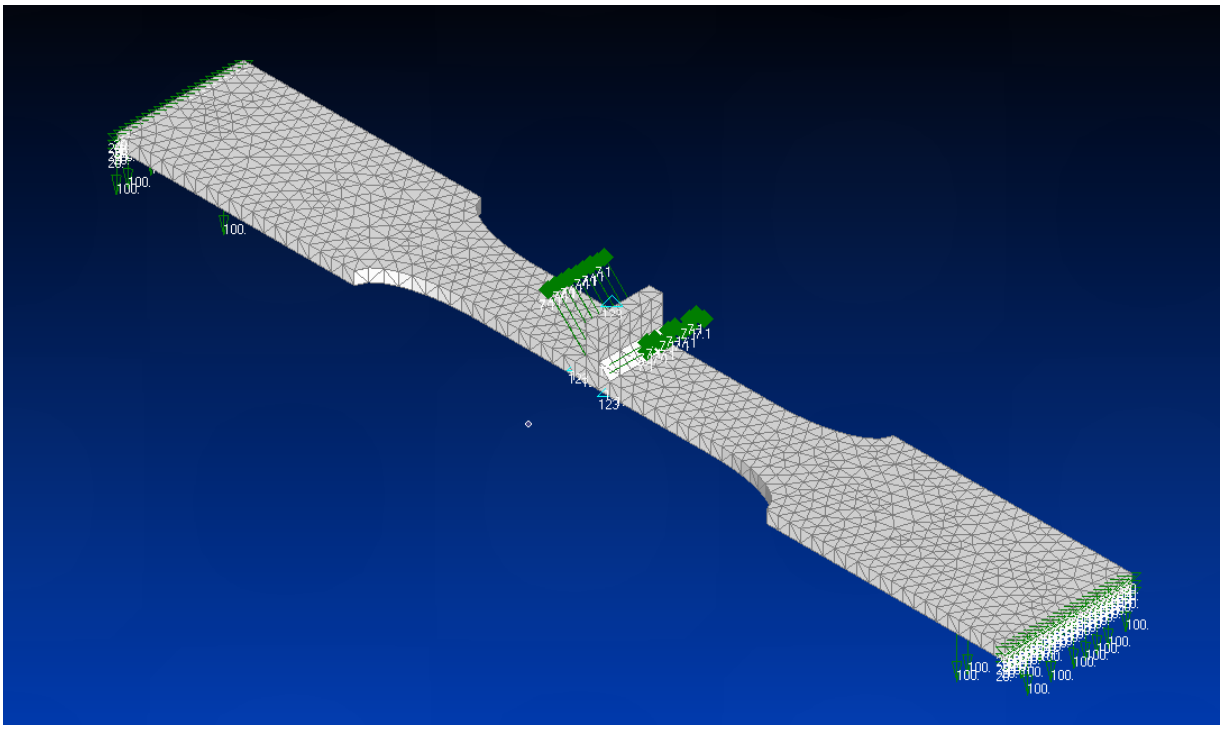

Figure 21. Mesh over the T-joint fillet weld

Later the mesh has been updated and refined for the material behavior model with the 52,649 number of elements.

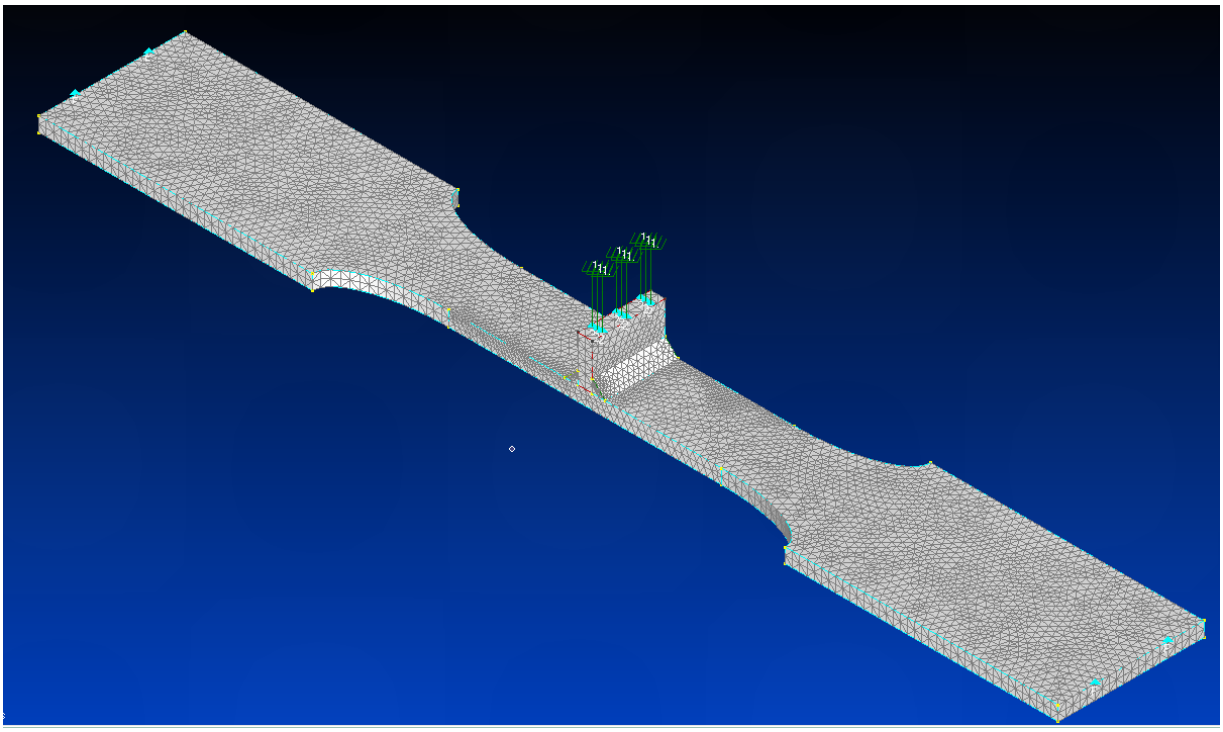

Figure 22. Refined mesh for material behavior model

5.5 Loads and constraints

As the purpose of this work is the study of residual stresses due to welding and preload so thermal load set have been chosen for the analysis. Heat flux value is calculated to be as follow

Heat flux = Heat energy / unit area = (0.8KJ/ mm^2 * 40mm) / (40mm * 11.2mm) = 7.1 KJ/mm^2

From the given heat energy value of 0.8 kJ/mm, heat flux value is calculated as it is heat energy per unit area. This thermal load is applied upon surface elements on the weld toe of the joint.

Constraints have been applied on the both ends of the weld specimen in all three translation directions e.g x, y, and z. additionally a reference temperature was necessary at the both ends of the specimen which is likely to be the room temperature. In this way we can see a temperature and heat distribution from the source. Without this reference temperature model gives an error.

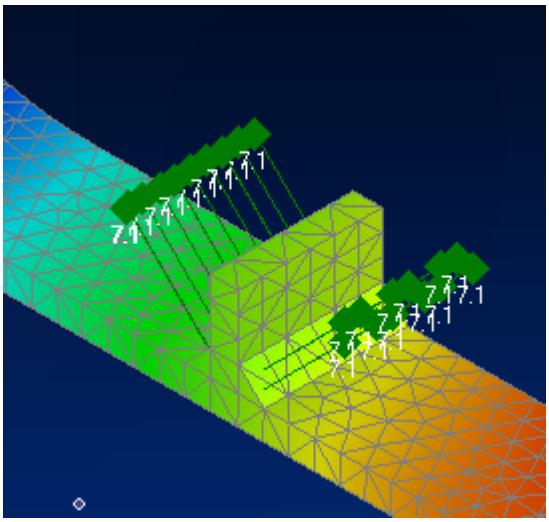

Figure 23. Thermal load application

5.6 Material behavior model

In the first case the calculations were carried out on linear model with the given material and prescribed thermal loads from welding. After this material behavior model was simulated for the nonlinear plastic behavior of the material. A function based on Ramberg-Osgood equation was made to get true stress-strain values and non-linear plastic model was formed depending upon this stress-strain function.

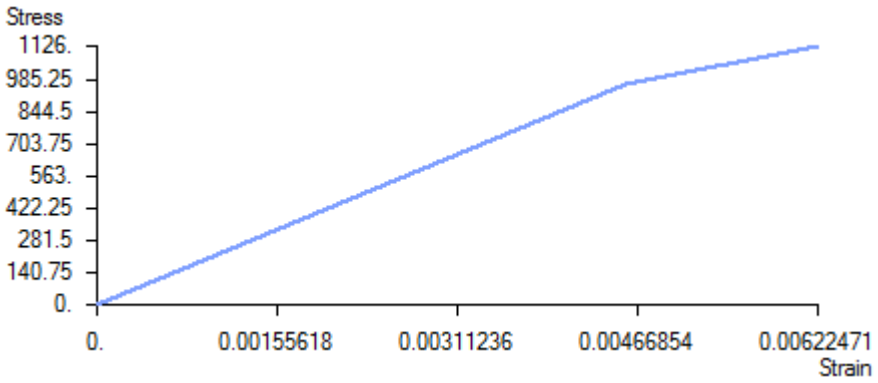

Figure 24. Stress-strain curve for material beahvior model

Material behavior is changing depending upon the material properties based upon this stress function and temperature. Analyses are done to calculate stresses using displacement control on the weld which cause a bending in the specimen. Figure 25 shows the material properties

changing with temperature. Here the values at room temperature have been multiplied with a factor K_θ to get the values at respective temperature.

$$E(T) = E° * K\theta$$

$$fy\,(T) = f° * K\theta$$

Where $E°$ and $f°$ are the values of elasticity modulus and yield strength at room temperatures. Figure 25 shows the variation of factor K_θ with temperature.

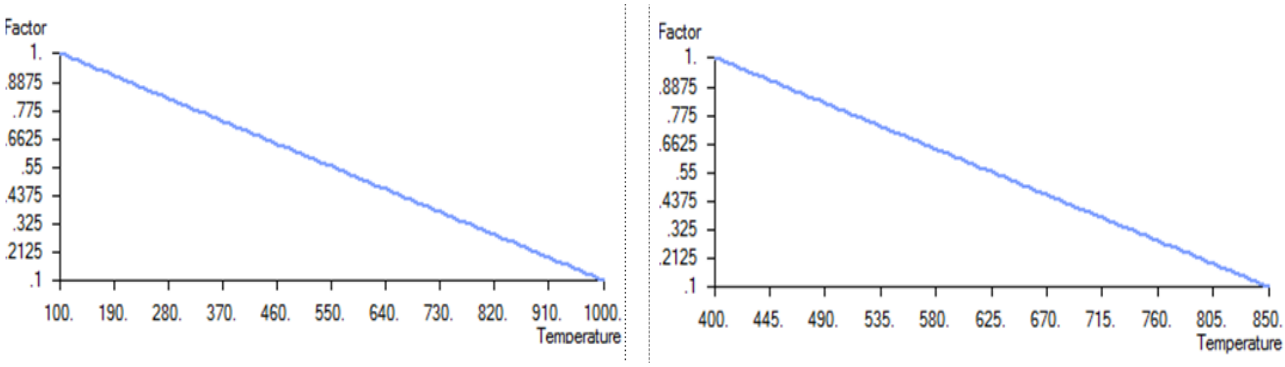

Figure 25. Factor by which elasticity modulus (left) and yield strength (right) changing with temperature

5.7 Results

After the steady state heat transfer and advanced non-linear analysis results have been taken from FE analyses on FEMAP. These results are showing different contours for stress and temperature at the T-joint. Temperature distribution on the weld specimen is shown in the following figure.

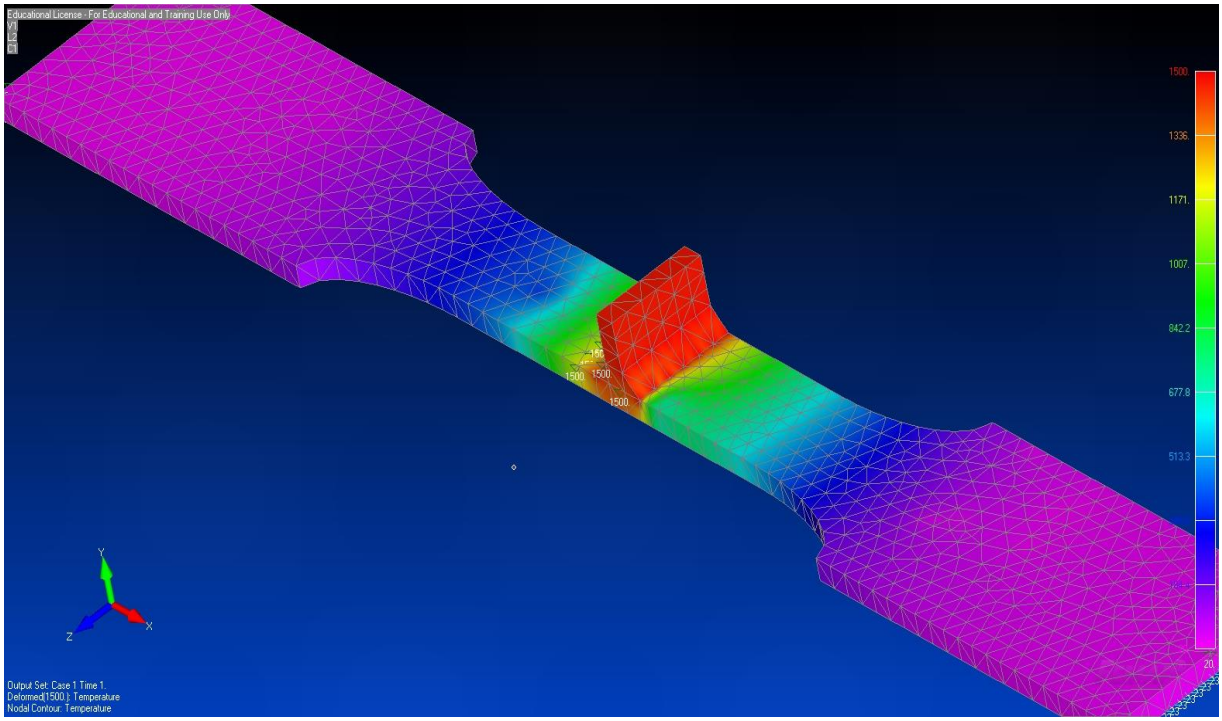

Figure 26. Temperature distribution during welding

Residual stresses were calculated using the heat input in the form of heat flux. From the results it has noted that the maximum stress area is the weld toe and near weld toe region. Material plasticity due to elevated temperatures has been taken care off in the model. Following figure shows the total translation in the specimen when thermal loads have been applied.

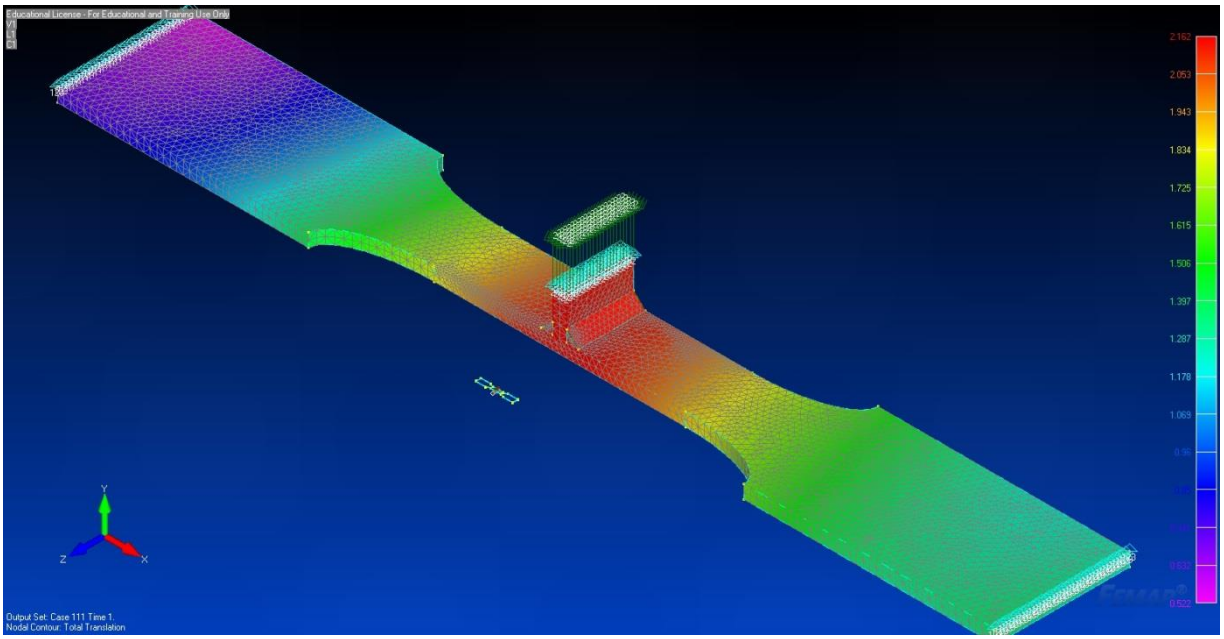

Figure 27 Total translation in T-joint under thermal loading

After modeling the T-joint for a linear analysis and predicting residual stresses material behavior model for the material under study (UHSS Optim 960QC) is simulated. The weld is studied again for residual stresses under displacement loading. The specimen is given a bending of 6 mm through displacement loading with constraints on both ends. A constraint in the direction of displacement is also necessary for the case. Figure 28 shows the stress distribution on the weld and it can be seen stresses are higher at the weld toe and near weld toe region. Figure 29 shows the weld toe of the T-joint fillet weld where the maximum residual stress region can be seen.

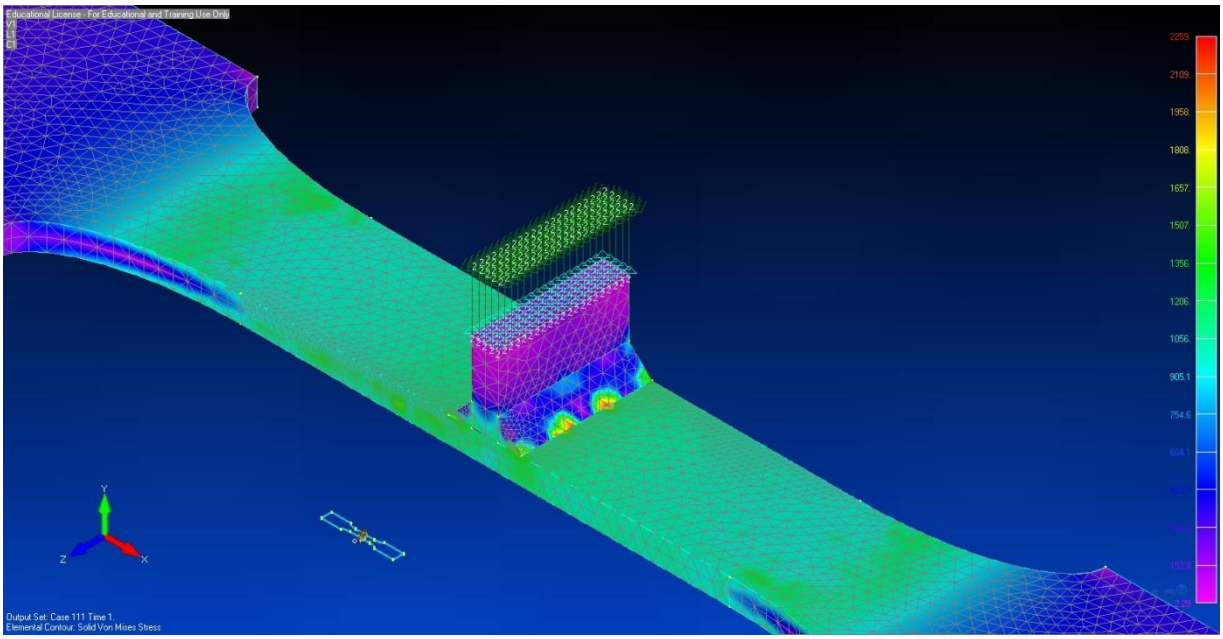

Figure 28 von Mises stresses in T-joint for the material behavior model

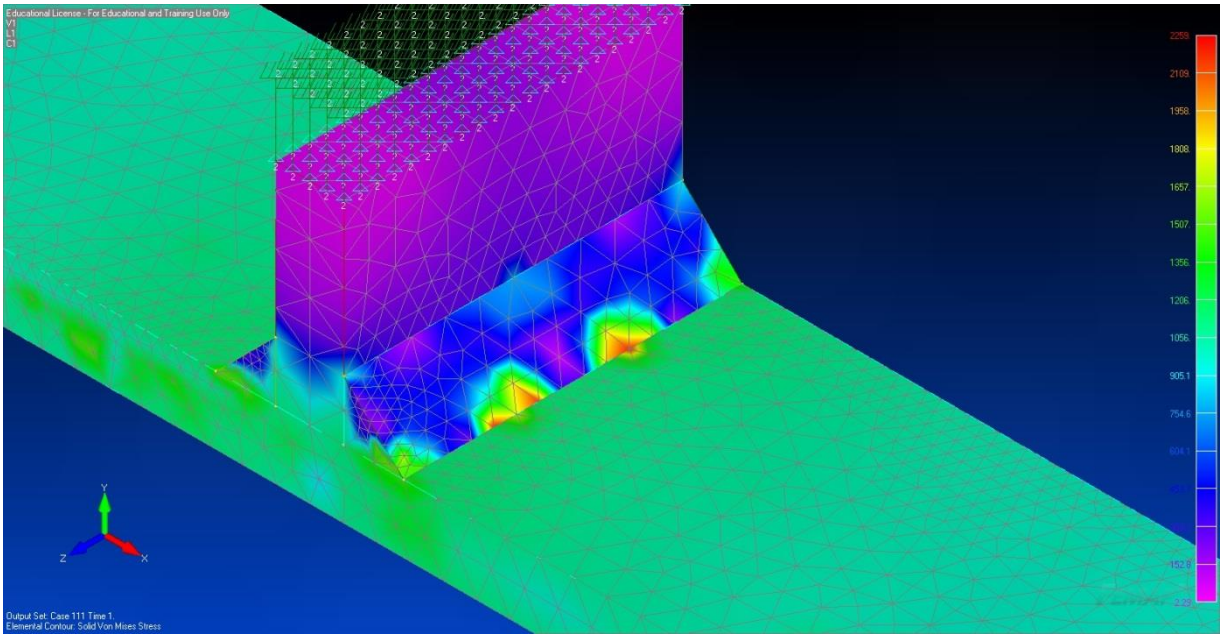

Figure 29 Weld toe of the T-joint material behavior model

Some more results have been taken from the simulated model. Following figures show the contours for x-direction normal stress and then Figure 30 shows the solid von Mises shear. Again shear values are higher in the weld toe region as expected.

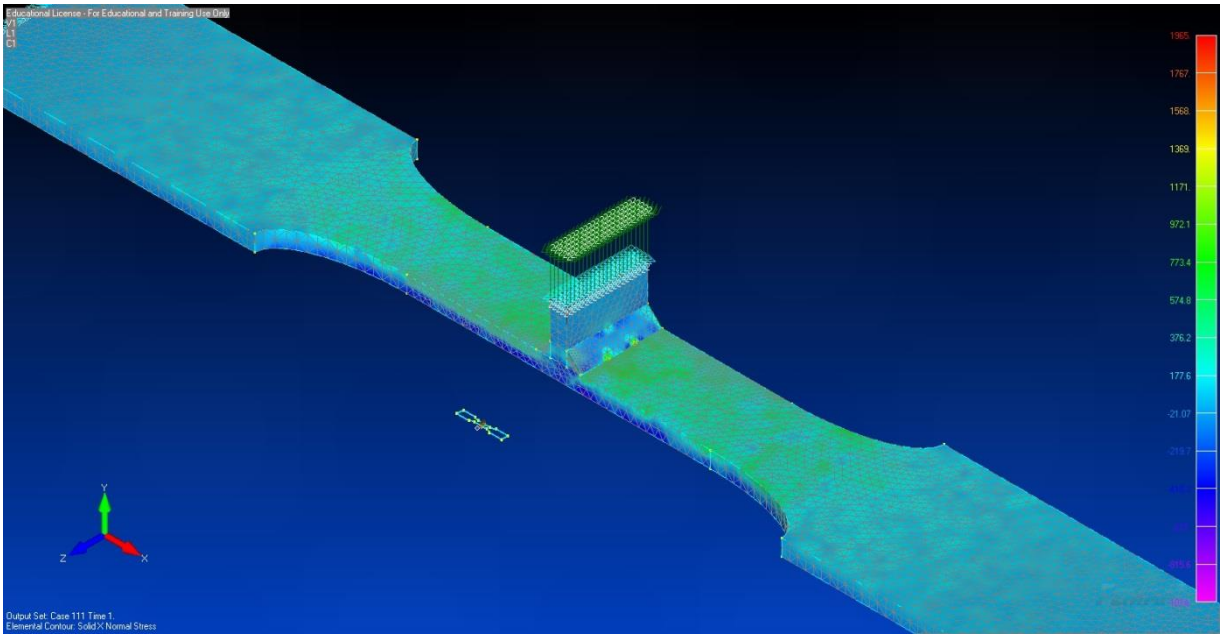

Figure 30. Solid x-direction normal stresses

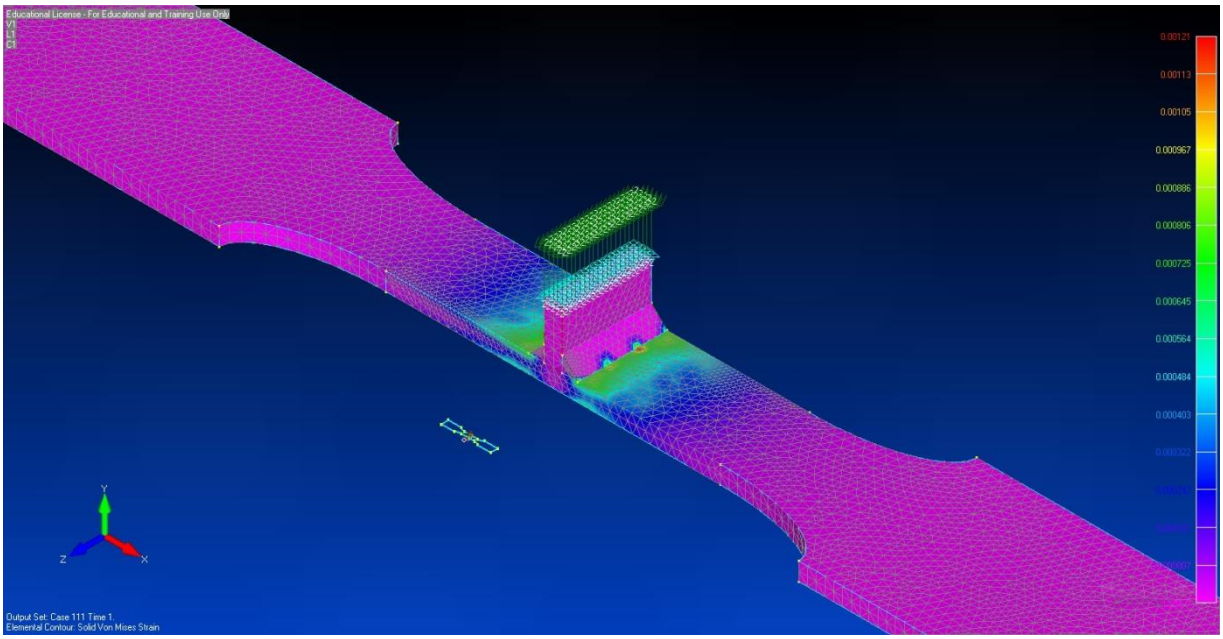

Figure 31. Solid Von Mises strain

The stress values are tabulated against time steps for the element 10945 in fist case of simulation which is thermal loading on elastic region for numerical analysis of the stress values.

Table 3. von Mises stresses for element 10945 on the weld toe for normal thermal loading

Time step	Stress Value MPa
1	0
2	0
3	0
4	0
5	16.80
6	0
7	0.08
8	35.62
9	0.05
10	0.05
11	0.05
12	0.05

13	0.05
14	0.05
15	0.05

The plot for the stress values in Table 3 has been shown in Figure 27

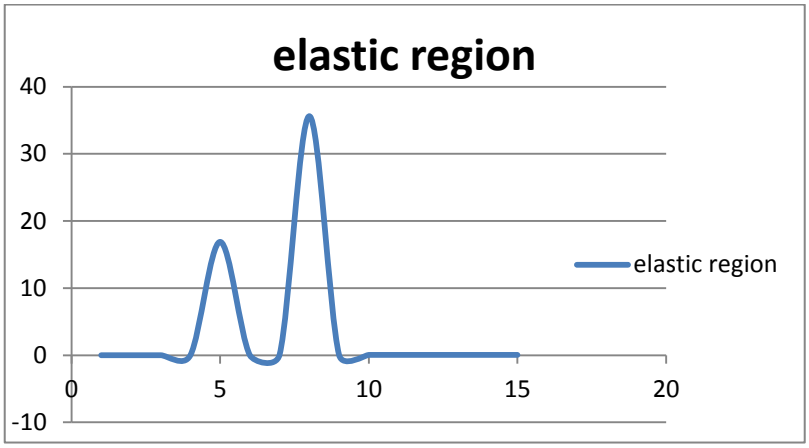

Figure 32 Plot for von Mises stresses in elastic region

The next table is giving the stress values for both elastic and plastic region. These are true stress values for material behavior model. Last 12 values of the time steps have been shown in the table

Table 4. von Mises stresses for the material behavior model

Time step	Stress Value MPa
783	1005
784	1007
785	1008
786	1010
787	1011
788	1012
789	1013
790	1015

791	1016
792	1019
793	1022
794	1025

These von Mises stresses of plastic region have been plotted in following Figure 28

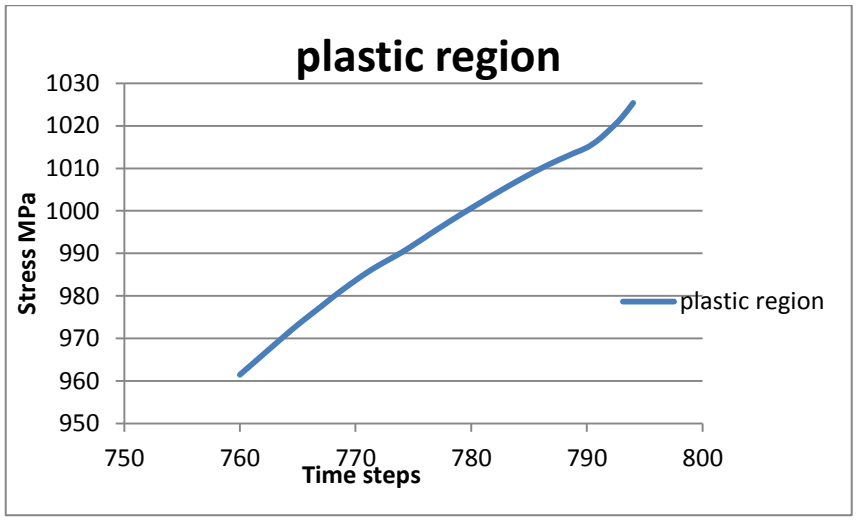

Figure 33 Plot of von Mises stresses for plastic region

5.8 Stress distribution plots

Stress distribution plots were obtained for three different elements on the specimen against time from the values got in Tables 1 and 2. The first graph is for normal linear behavior model. The location of element 1 is at the place where strain gauge was mounted on the surface of the plate, the element 3 is between the middle of plate and element 2 is on the weld toe. It is clear that the stress values are maximum for the element at the weld toe than at the plate surface and middle of the main plate.

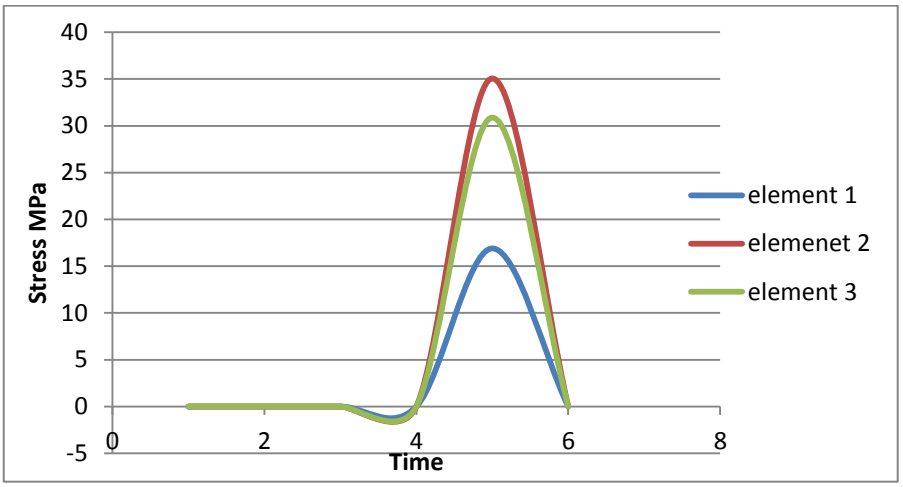

Figure 34. Stress distribution for three different elements at three different locations

The next graph is representing the stress distribution of material behavior model. Here the stress values are almost same for all three elements except a little change during welding.

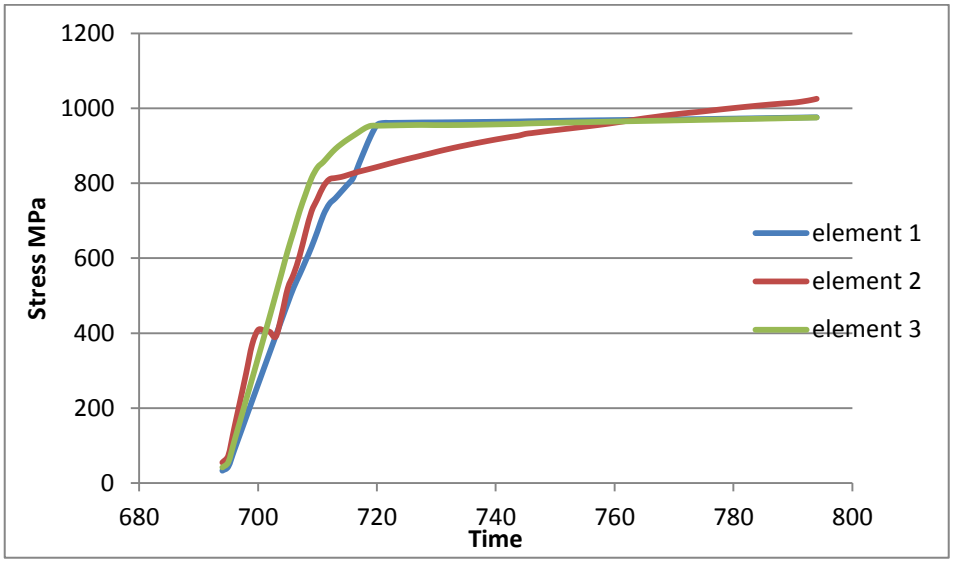

Figure 35. Stress distribution for material behavior model

The residual stress distribution over the plate thickness at the weld toe is shown in next Figure 36

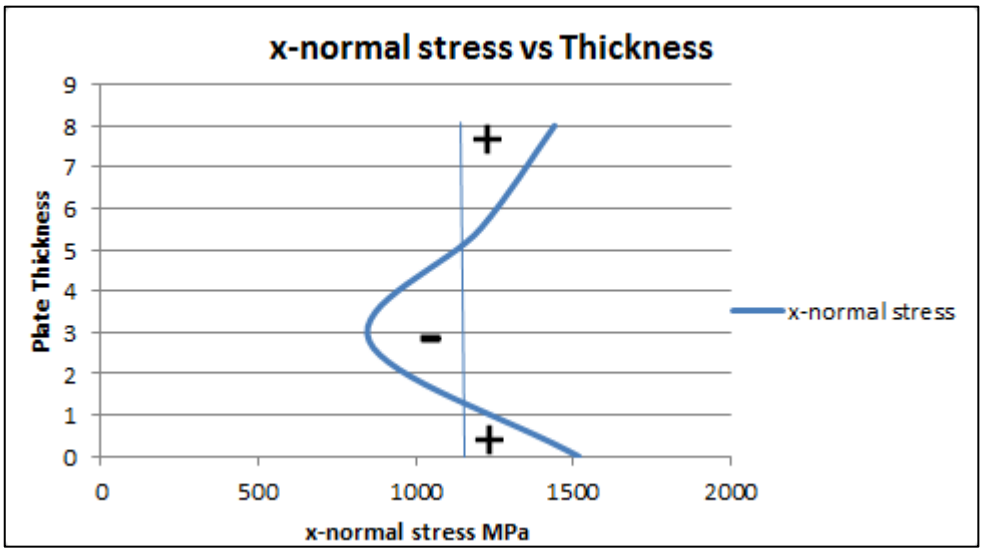

Figure 36. x-normal stress distribution over the plate thickness

Figure 39 shows the stress distribution lines over the joint from y = 0 to y = 8mm. This is because of our boundary conditions. If there is no force or support at the ends of joint average stress value in cross section would be zero

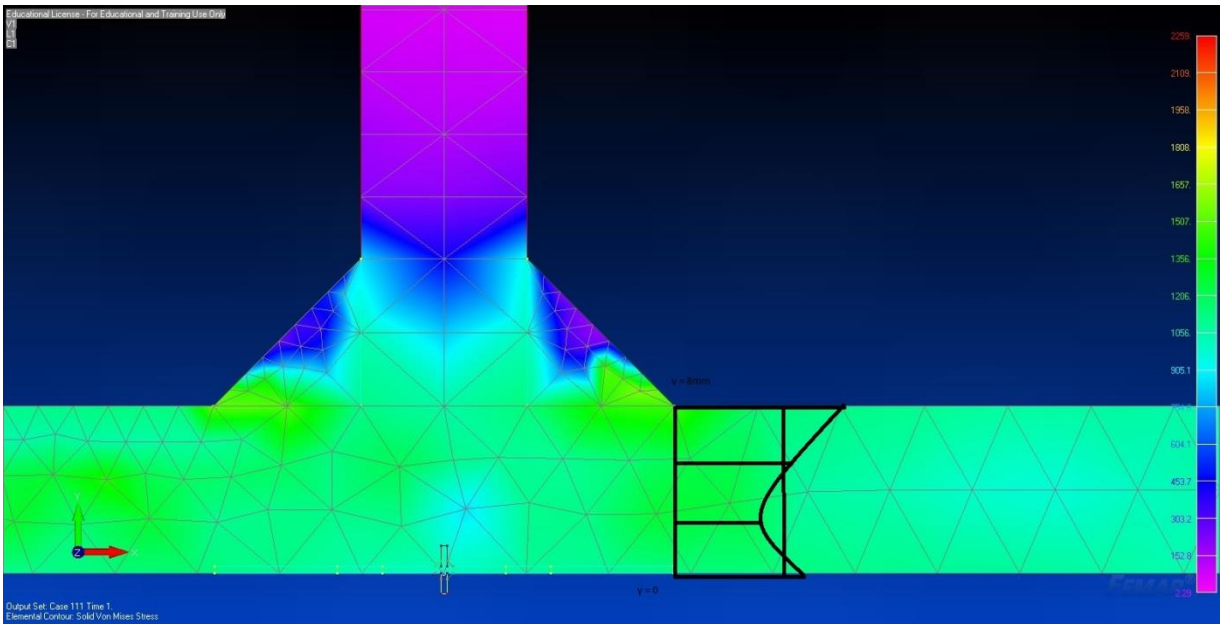

Figure 37 Side view of the joint showing stress distribution lines

5.9 Residual stress at the weld toe calculated by temperature reaction force

Residual stress on the weld toe is calculated by reaction force due to heat as follow

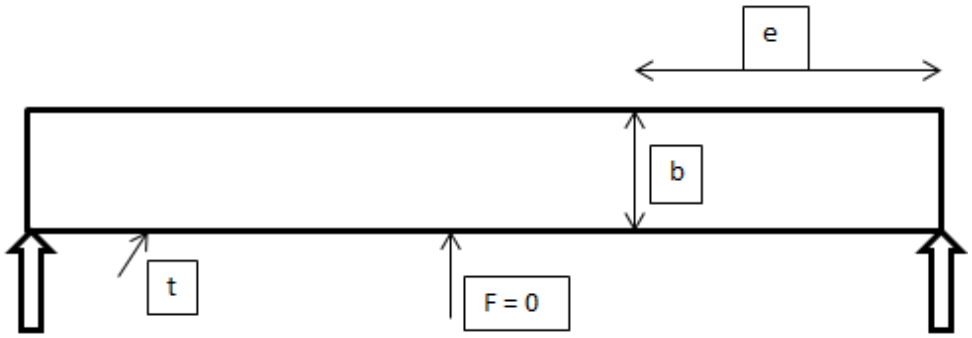

Figure 38. Schematic diagram for the calculation of reaction forces on the plate

Change in strain before and after the welding is $\Delta \in$

$\Delta \in = 0.004$

$$\Delta R = E\ b\ t^2 \frac{1}{6e\ (1 - \gamma 2)}$$

Where ΔR_{total} = change in total reaction force

E = Modulus of elasticity

b = width of plate

t = thickness of plate

e = distance of the edge from the strain gauge mounted on the plate

γ = Poisson's ratio

ΔR_{total} = 210000 *40 * 8^2 / 6*219* (1-0.33^2)

ΔR_{total} = 183.65 N

$$\Delta R(total) = \Delta R(T) + \Delta R\ (G)$$

$$\Delta R_T = \Delta R_{\ total} - \Delta R_G$$

ΔR_T = 183.60 N

This reaction force has been employed on the FE model to calculate the residual stresses on the weld toe. The maximum value of von Mises stress for and element at the weld toe calculated by this method is 985 MPa, and the maximum x normal stress is 332 MPa. This value is quite near to the x normal stress calculated experimentally.

6 Discussion

Residual stresses and distortions are unavoidable in welding and their effects cannot be disregarded. They occur near the T-joint due to localized welding and subsequent rapid cooling. They increase or decrease the fatigue strength by affecting the crack growth rate. Residual stresses can have a significant effect on fatigue performance of the welded joints. A fatigue crack has poor growth under a predominantly residual stress field. Both initial residual stress state and subsequent residual stress relaxation need to be considered for accurate description of fatigue behavior.

Validated methods are required for predicting welding stresses and distortions due to complexities in welding process like localized heating, temperature dependence of material properties, and heat source. Many researchers have predicted the thermal and mechanical responses in weldments both theoretically and experimentally leading ways to eliminate unfavorable deformations. Studies have shown both thermal and mechanical models. In mechanical analysis, thermal loading was used as input obtained from temperature history of thermal analysis. Thermal stresses are calculated from temperature distribution of thermal model for each weld pass. A stress acting normal to the direction of the weld bead is known as transverse residual stress, denoted by σ. Stress acting parallel to the direction of weld bead is known as longitudinal residual stress. Empirical and simulation methods were used in this research for the analysis of welded joints.

In the experimental part the stresses were measured 50 mm away from the weld toe as it is practically impossible to implant strain gauges un the weld toe. The strain gauges on both sides of the weld toe measure the x-direction stresses. Both the gauges show almost the similar kind of stress behavior. At the beginning this 350 MPa came from the preload. Then there was the first welding part (approx. time step 300) and after first welding the stress value decreased to 270 MPa. The second welding was done at time step 2400 (see the peak value) and after that stress values returned back to 270 MPa. At the end preload was released and stress value dropped to exactly zero. Temperature measurements taken by the thermocouple at the weld toe shoes a maximum value of 1100 °C and it decreases to room temperature value during cooling of welds.

In FE analysis part both linear and nonlinear analysis has been performed. The resulting stresses were due to thermal loading which is applied as heat flux. Temperature and stress contours have been displayed in FE analysis results section. The temperature values are maximum at the weld toe as expected. The stress values also reach their maximum values at and near weld toe regions.

If we compare the experimental measurements and FE analysis results they show similarity to each other in both temperature and stress values. Temperature graphs from the experimental part and the temperature contour in FE model both shows the temperature variation between 1100 to 1200 °C near weld toe regions. For the comparison of stress values from experimental and FE analysis, we can compare the graphs for x-direction normal stresses. The stress contours for material behavior model are higher than in the normal case. There is a decrease in stress with and axial load on the specimen according to FE model which is also confirmed by the experimental results.

A comparison of x-direction normal stress distribution plot of experimental results and FE results have been shown in the following figure.

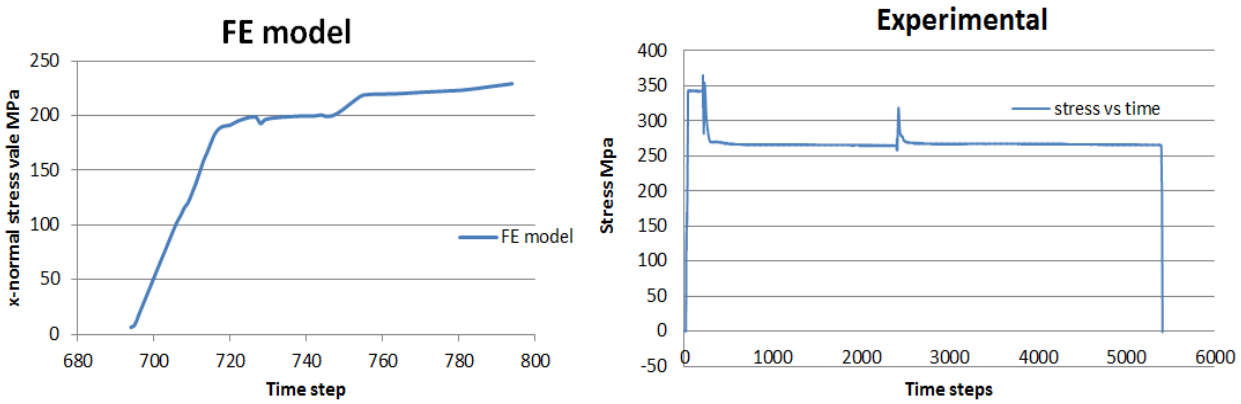

Figure 39. Comparison of X-direction normal stresses from experimental and FE analysis part

In FE-model plot the welding starts nearly from the 750th time step. It can be noted that there is a difference of 100 MPa in the peak value of x-direction normal stress from experimental and FE model. This difference is due to the change in input energy which is 1 KJ/mm in experimental part and 0.8 KJ/mm in FE model simulations. Secondly stresses from experimental part are showing gradual increase and decrease in the stress level but in case of FE model variation in stress levels is quite random. In contrast the von Mises stress plots show gradual and smooth variations from FE model as well in Figure 34 and Figure 35.

7 Conclusions

Validated methods for predicting welding stresses and distortion are required because of the complexity of welding process, which includes localized heating, temperature dependence of material properties and heat source.

Residual stresses are occurring due to preventing the free shrinkage of weld and base material around it. Distortion occurs due to shrinkage which can take place partly. Residual stresses increases with increasing flange thickness, while they decrease near the fillet weld toe by increasing heat input.

Residual stresses can have a significant effect on fatigue performance of the welded joints. Both initial residual stress state and subsequent residual stress relaxation need to be considered for accurate description of fatigue behavior.

Experimental setup revealed the growth pattern of stress in the specimen. There are stresses with the preload without welding. Then during welding stress start increasing and reaches its maximum level, after that they maintain a steady level and starts dropping to initial values during cooling of the weld. The temperature increased to 1100 °C during welding.

Thermal loads have been used in the form of heat flux in FE analysis. Results and stress contours shows that the maximum stress area is the weld toe and near weld toe region. Residual stresses decrease if we apply a bending load at the end of the specimen during welding.

Stress distribution plots show stress values for three different elements at three different locations. The element near the weld toe has the maximum value than the element in middle of plate and at the place where strain gauge was mounted. Residual stresses calculated by reaction force at the weld toe are approximately same as calculated in experimental work

Experimental results show quite a good agreement with the FE analysis results.

Bibliography

[1] Teng, Tso-Liang, C.-P. Fung, P. H. Chang and W.-C. Yang, "Analysis of residual stresses and distortions in T-joint fillet welds," *International Journal of Pressure Vessels and piping,* no. 78, pp. 523-538, 2001.

[2] Z. Barosum and I. Barosum, "Residual stress effects on fatigue life of welded structures using LEFM," *Engineering failure analysis,* vol. 1, no. 16, pp. 449-467, 2009.

[3] Ruukki, 27 03 2013. [Online]. Available: http://www.ruukki.com/optimqc. [Accessed 28 03 2013].

[4] T. Kumose, T. Yoshida, T. Abbe and O. H, "Predicting of angular distortion caused by one-pass fillet welding," *Welding Journal,* vol. I, pp. 945-56, 1954.

[5] M. a. DeBiccari, "Prediction of welding distortion," *Welding Journal,* vol. I, pp. 172-81, 1997.

[6] J. Arnold, R. FD and P. Goff, "Predicting residual stresses in multi-pass weldments with finite element methods," *Coompt Structure,* vol. 2, no. 32, pp. 365-78, 1989.

[7] D. Finch and F. Burdekin, "effect of welding residual stresses on significance of defects in various types of welded joints," *Engineering Fracture mechanics,* vol. 5, no. 41, pp. 721-35, 1992.

[8] N.-X. Ma, Y. Ueda, H. Murakawa and H. Maeda, "FEM analysis of 3D welding residual stresses and angular distortion in T-type fillet welds," *Trans Jpn weld Res Institute,* vol. 2, no. 24, pp. 155-122, 1995.

[9] I. B. Z. Barsoum, "Residual stress effects on fatigue life of welded structures using FEM," *Engineering failure analysis,* no. 16, pp. 449-467, 2009.

[10] Nitschke-Pagel and H. Wohlfahrt, "The generation of residual stresses due to joining process, Resiudal stress measurement, calculation and evaluation," *DGM-informationsgesellschaft Verlag,* vol. 1, pp. 121-134, 1991.

[11] M. Farajian, "Welding residual stress behavior under mechanical loading," in *Commission XIII Fatigue of welded components and sructures, International Institutes of Welding* , Paris, 2012.

[12] G. Glinka, "effect of Residual stresses on Fatigue crack growth in steel weldments under constant and variaböe amplitude loads," in *Fracture Mechanics*, American Society for testing and Materials, 1979, pp. 198-214.

[13] C. Y. Chen, Fatigue and Fracture, Huazhong Univeristy of Science and Technology, 2007.

[14] Z. Barsoum, "Fatigue design of welded structures- effect of weld quality and residual stresses," Internationlal Institute of Welding IIW, Sweden, 2010.

[15] P. Lingyun, A. Badrinaryan, F. James A, W. Huang, L. Zhang, W. Li, U. William and M. Justin C, "welding residual stress impact on fatigue life of a welded structure," *International institute of welding,* vol. 1, no. XIII-2420-12, pp. 2-3, 2012.

[16] C. Lilijedhal and O. Zanellato, "The effect of weld residual stresses and their redistribution with crack growth during fatigue under constant amplitude loading," *Internal Journal of Fatigue,* vol. 1, no. 32, pp. 735-743, 2010.